nature portfolio

Peer Review File

Metasurface Enabled High-order Differentiator

Corresponding Author: Professor Din Ping Tsai

This file contains all reviewer reports in order by version, followed by all author rebuttals in order by version.

Version 0:

Reviewer comments:

Reviewer #1

(Remarks to the Author)
This manuscript presents a novel approach to optical analog differentiation using a Pancharatnam-Berry (PB) phase metasurface to achieve high-order differentiation in optical imaging. By leveraging phase-gradient designs and integrating the metasurface into a 4f imaging system, the authors achieve up to fifth-order differentiation and demonstrate applications in edge detection and optical super-resolution. The manuscript is technically strong, well-organized, and has a substantial potential impact in fields such as biomedical imaging, microscopy, and semiconductor manufacturing. Therefore, I would recommend its publication once the following comments are properly addressed.
• In the manuscript, the authors demonstrated the differential imaging up to fifth-order. What is the limit of the high-order differentiation in the proposed methodology?
• It seems the differential imaging has limited working areas (0.5 mm ≥ x ≥ – 0.5 mm), which may affect the real application. Generally how to enlarge the working areas?
• For higher-order optical differentiation, the contrast between discrete intensity peaks becomes worse as shown in Fig. 3n-s. What is the origin of this? How to improve the contrast?
• To highlight the novelty of this work, I suggest the authors give a comparison between this work and other works of spatial differentiation.
• I wonder if high-order differentiation can be achieved in two dimensions using the proposed method.

Reviewer #2

(Remarks to the Author)
The authors utilize a PB phase metasurface placed at the Fourier plane of a lens system to modulate the Fourier spectrums and realize differentiators of high orders. They experimentally demonstrate a 5th-order differentiator and used the method for detecting two closely spaced laser sources as an example of its potential applications. Several issues for the authors to check:

1) The manuscript stated “However, most previous works primarily focused on the first- and second-order operation. A fundamental challenge remains as to how to realize the high-order operation” (line 19 to 21), and it derives a universal formula, t(k_x,k_y)=(ik_x)^n (ik_y)^m. However, such high-order differentiator has already been fully studied and reported before, for example, in Nat. Commun. (2024) 15:2237, and a universal formula has been reported for arbitrary-order differentiators and their combinations, namely, t(x,y)=∑_(j=1)^l▒[C_j (-ix)^(m_j) (-iy)^(n_j)] , in which x is the coordinate at the Fourier plane, equivalent to kx in the formula presented in the manuscript. The Nat. Commun. 2024 paper also demonstrated a fourth-order differentiator in theory and simulation and used the same 4f system and Si metasurface. The novelty of the work needs to be clarified, and the claim needs to be reconsidered.

2) The reported work achieved a 5um lateral resolution at NA=0.001 and stated that it is two orders of magnitude improvement over conventional method in photolithography. The alignment accuracy of photolithography machine can easily achieve tens of nm resolution and even single digit resolution for the advanced tool, far better than 5um. The authors postulate the method discussed could achieve nm scale resolution if a high NA imaging system is used. It is recommended the author show such a high NA system to support the claim, as this is one of the key applications of this technology and the situation in high NA is very different from very small NA.

3) It is claimed that two independent lasers are treated as incoherent, however, formulars (5)-(7) are derived on and only

valid for two coherent light sources. Please explain.

4) In Figure 4b, even at d=0, there is already measurable value of 1st and 3rd order differentiators. Please explain it.

5) For Figure 4c, please elaborate what each of the 5 layers could be and how they are correlated to the measurement system showed in Figure 4a. In real application, considering the substrate could be non-transparent (e.g. Si) or with other existing patterns and with large thickness, a reflective optical system is more practical

6) The current super-resolution experiment is based on two lasers with already known and fixed intensity and beam waists. In real situation, the intensity and number of point objects are un-known. How would these affect the effectiveness of the current method?

7) What is the reason to have PMMA baked for 1 hour, which is much longer than the conventional practice of just several minutes? Why K9 glass is chose as the substrate?

Reviewer #3

(Remarks to the Author)
I co-reviewed this manuscript with one of the reviewers who provided the listed reports. This is part of the Nature Communications initiative to facilitate training in peer review and to provide appropriate recognition for Early Career Researchers who co-review manuscripts.

Reviewer #4

(Remarks to the Author)
This manuscript proposes a high-dimensional differentiation (i.e., "cascaded" edge detection) of optical images using a Si metasurface multiplexed to provide different orders through different diffraction channels. It claims an experimental demonstration of all-optical differentiations up to the fifth order based on a simple intensity object and a phase object. Pancharatnam-Berry phase allows for broadband operation. More interesting aspect of the paper is the potential utilization of differentiation to detect short separations between two objects beyond the Rayleigh limit. With this approach they can detect a separation of 5 um, which is comparable to the pixel size.

For this paper to be published in Nature Communications, the authors should better highlight the novelty and the limits of their technique. It’s been mentioned that all-dielectric multilayer structures are used for high-order differentiation, but the present manuscript argues a general design strategy. Although mathematical form of high-order differentiation is given (unfortunately with some confusion), the design strategy is not well described for metasurfaces for an arbitrary order. Also, the manuscript only investigates 1D filtering. There is an error or confusion in the manuscript as for how an arbitrary order differentiation is defined even mathematically. The partial derivatives on the left hand side of Eq. 2 is not equal to the one given in the next line after Eq. 2. Also, what are the limitations of the present implementation with metasurfaces? How far can it go in terms of differentiation order? What are the theoretical and practical limitations (metasurface related, detection related, etc.)? One of the important motivations of using metasurfaces is the miniaturization especially in the direction of optical axis. Is it really feasible to combine the functions of other optical components, lenses (e.g., Fourier transform, etc.) with the metasurface while preserving high-order differentiation functionality? Are there any other unique applications besides super-resolution detection of two point sources?

Given that minimum detected separation is 5 um, (i.e., already comparable to pixel size), what type of advantage would high NA system provide, without having higher resolution camera?

In Fig. 3h, although a phase object is used for differentiation, the main impact is not really coming from the phase distribution. The edge detection is still effective on the sharp intensity variations at the outermost boundary of the square (i.e., see the black square outline). Therefore, this figure does not really seem to demonstrate differentiation on phase distribution. What’s the intensity contrast between the interior of the square and the black outline?

What’s the new information we learn from the differentiated images vs bright field images in Supplementary Fig. 1? What’s the advantage in differentiation?

Although the two Gaussian beams are incoherent wrt each other, Eqs. 5 and 6 don’t seem to treat them correctly as incoherent beams. It’s interesting, then, why the theoretical curves in Fig. 4 agree with the experiment.

Minor comments: The manuscript has many grammatical errors. Some texts in some figures are not legible.

Version 1:

Reviewer comments:

Reviewer #1

(Remarks to the Author)
I am very satisfied with the efforts the authors made to improve the manuscript. The significantly revised manuscript can be accepted as is.

Reviewer #2

(Remarks to the Author)
The authors have responded to all my comments and made revisions accordingly in the manuscript. The paper is in much better shape now. Only one more point for the authors to check:
It is shown by the authors that not only the relative distance between the two lasers (d=d1-d2) but also the absolute distances between these lasers and the metasurface (d1, d2) are important. And it is said that the laser 1 is firstly aligned with the metasurface, namely d1=0. I am concerned about the accuracy of this preconditional alignment of laser 1 and the metasurface. Could the author deliberately set d1≠0 and be comparable to d2 (i.e. d1~= d2), and then check whether equation R1 or R2 is still the right formula?

Reviewer #3

(Remarks to the Author)
I co-reviewed this manuscript with one of the reviewers who provided the listed reports. This is part of the Nature Communications initiative to facilitate training in peer review and to provide appropriate recognition for Early Career Researchers who co-review manuscripts.

Reviewer #4

(Remarks to the Author)
I have reviewed the revised manuscript and don't have additional comments.

Version 2:

Reviewer comments:

Reviewer #2

(Remarks to the Author)
The authors have addressed the comments raised.

Reviewer #3

(Remarks to the Author)
I co-reviewed this manuscript with one of the reviewers who provided the listed reports. This is part of the Nature Communications initiative to facilitate training in peer review and to provide appropriate recognition for Early Career Researchers who co-review manuscripts.

Reviewer 1:

General Comment:

This manuscript presents a novel approach to optical analog differentiation using a Pancharatnam-Berry (PB) phase metasurface to achieve high-order differentiation in optical imaging. By leveraging phase-gradient designs and integrating the metasurface into a 4f imaging system, the authors achieve up to fifth-order differentiation and demonstrate applications in edge detection and optical super-resolution. The manuscript is technically strong, well-organized, and has a substantial potential impact in fields such as biomedical imaging, microscopy, and semiconductor manufacturing. Therefore, I would recommend its publication once the following comments are properly addressed.

Response:

We thank Reviewer for the positive recommendations and instructive suggestions. We have followed all of the suggestions to revise our manuscript. The main changes include:

1) In Principle, we have added some descriptions to reveal how to enlarge the working area;
2) In Supplementary information, we have added two new sections to discuss the limit of high-order differentiation and high-order differentiation in two dimensions.

By addressing the concerns, we indeed feel that our manuscript has been much improved now, and we sincerely wish Reviewer could consider the manuscript for publication in Nature Communications.

Specific Comments:

1. In the manuscript, the authors demonstrated the differential imaging up to fifth-order. What is the limit of the high-order differentiation in the proposed methodology?

2. It seems the differential imaging has limited working areas (0.5 mm ≥ x ≥ − 0.5 mm), which may affect the real application. Generally how to enlarge the working areas?

Response:

We would like to answer the above comments together. It is very instructive for Reviewer to point out these questions. Based on the differentiation property of the Fourier transform, in order to realize the *n*-order differentiation operation in real space, we just need to construct a complex amplitude filter, $(ik)^n$, in Fourier space. In our manuscript, by designing the phase gradient of the Pancharatnam-Berry (PB) metasurface as, $\phi_n(k) = c_n k^n$, with c_n being a constant to ensure that $\phi_n(k_x)$ is sufficiently small, we construct the aforementioned complex amplitude filter. Specifically, we illuminate the PB metasurface with a horizontally polarized light, $A(k)$, then we select the vertical component, i.e., LCP-RCP, from the output light field. Accordingly, the light field at the Fourier plane can be equivalently expressed as, $E = [exp(i\phi_n(k)) - exp(-i\phi_n(k))]A(k) \propto sin(\phi_n(k))\,A(k)$. By leveraging the basic principle of Taylor's expansion, if $\phi_n(k)$ is a small value, the light field at the Fourier plane can be simplified as, $E \propto \phi_n(k)A(k)$. In our experiment, we select the $c_1 = 1.04 \times 10^3$, $c_2 = 2.2 \times 10^6$, $c_3 = 4.66 \times 10^9$, $c_4 = 9.55 \times 10^{12}$, $c_5 = 2.03 \times 10^{16}$, and thereby, the approximation $sin(\phi_n(k)) = sin(c_n k^n) \approx c_n k^n$ holds true only within a limited region, namely, **the differential imaging has limited working areas, as indicated in Comment 2 by Reviewer. In order to enlarge the working areas, we only need to reduce the value of c_n to ensure that the approximation holds over a wider range.** We have clarified this point in our revision. (Seen on Page 7 in the main text)

"For demonstration, here, we set $c_1 = 1.04 \times 10^3 m^{-1}$, $c_3 = 4.66 \times 10^9 m^{-1}$, and $c_5 = 2.03 \times 10^{16} m^{-1}$, for realizing first-, third-, and fifth-order differentiation operation, and the corresponding phase gradients are illustrated in Fig. 1. As shown in Fig. 1a, for the particular case with $n = 1$, which is the commonly used linear gradient phase for edge detection or first-order differentiation operation[23]. As shown in Fig. 1b and Fig. 1c, we can easily prepare the required optical transfer function for realizing high-order differentiation. Note that, based on the principle of Taylor's expansion, $E_{\mathcal{F}}$ can be approximated as $(k_x)^n A(k_x)$ only at a limited working area, as indicated by the region between black dashed lines. In order to enlarge the working areas, we can reduce the value of $\boldsymbol{c_n}$"

Furthermore, the aforementioned gradient phase construction also offers a scalable approach for implementing higher-order differential operations, **corresponding to Comment 1 by Reviewer. By selecting the suitable value of c_n, one can realize arbitrary order differentiation. In this regard, there are no limits to the differentiation order in theory.** However, for most functions, as the order of differentiation increases, the signal strength typically diminishes, which places higher demands on the detector's response. Additionally, the phase gradient of the metasurface for realizing higher-order differentiation rises exponentially, requiring more precise alignment, which is also indicated in Fig. 4b. Therefore, higher alignment accuracy is essential to achieve reliable results for high-order differentiation in practical experiments. Furthermore, orthogonal polarization filtering is required in our scheme, which also reduces the intensity of the differentiation signal. Inspired by Reviewer 1 and Reviewer 4, we have added a new section in Supplementary information to clarify this point. (Seen on Pages 5-7 in the Supplementary information)

"Supplementary Note 4. The numerical simulation of high-order differentiation operation

The proposed scheme can be extended to embrace arbitrary order differentiation operation merely by setting a suitable gradient phase of the PB metasurface. Specifically, by selecting the value of c_n, one can ensure that $E_{\mathcal{F}}$ (Eq. (3) in the main text) can be approximated as $(k_x)^n A(k_x)$ within a specific working region, thereby, enabling the arbitrary order differentiation operation. Here, as a reference, we design and optimize the parameters required for the 6th to 10th-order differentiation operations. As shown in Supplementary Fig. 4, we use a Gaussian beam as the input and achieve its higher-order differentiation operations by employing the optimized parameters, c_n. The corresponding c_n required for each order are listed in the upper left corner of each figure. The parameters of the unit cell are consistent with those described in the main text. The separated lobes in Supplementary Fig. 4 are consistent with the theoretical predictions indicated by $\frac{\partial^n G(x,y)}{\partial x^n} \propto G(x,y) H_n\left(\frac{x}{\sqrt{2\sigma^2}}\right)$ (seen in the main text), which implies that our approach can be extended to higher orders. However, for most functions, as the order of differentiation increases, the signal strength typically diminishes, which places higher demands on the detector's response. Additionally, the phase gradient of the metasurface for realizing higher-order differentiation rises exponentially, requiring more precise alignment, which is also indicated in Fig. 4b in the main text. Therefore, higher alignment accuracy is essential to achieve reliable results for high-order differentiation in practical experiments. Furthermore, orthogonal polarization filtering is required in our scheme, which also reduces the intensity of the differentiation signal.

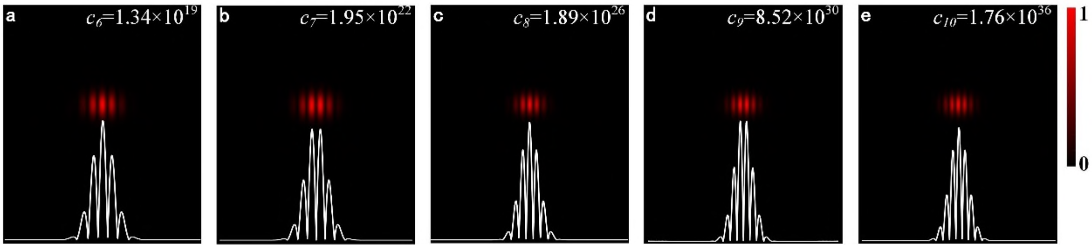

Supplementary Fig. 4. Numerical simulations for the high-order differentiation. a-e correspond to the differentiation of Gaussian input from 6th to 10th-order. The white lines therein represent the intensity distributions along the center of the red patterns. The unit m^{-1} for c_n at the top-right corner is omitted."

3. For higher-order optical differentiation, the contrast between discrete intensity peaks becomes worse as shown in Fig. 3n-s. What is the origin of this? How to improve the contrast?

Response:

We thank Reviewer for this insightful comment. Actually, the higher-order optical differentiation of the square is similar to that of the Gaussian mode. Although the n-order differentiation produces n+1 peaks, the peak intensity decreases from the center toward the edges, which can be seen clearly in above Supplementary Fig. 4. Here, we take the high-order differentiation of a one-dimensional rectangular function, corresponding to the square in Fig. 3, as an example to illustrate this point to Reviewer. As shown in Fig. R1, we calculate the first to fifth-order derivatives of the left edge of the rectangular function (marked by the blue circle in Fig. R1a). The corresponding results are plotted in Fig. R1b-f. As we know, the n-order derivative of a function can be viewed as the first-order derivative of its (n−1)-order derivative. Taking the second and third-order derivatives as examples, as indicated in Fig. R1c and d, since the gradient in the central region of the second-order derivative is steeper than that in the edge regions (marked by blue arrows), its derivative, i.e., the third-order derivative, results in the central peak having a higher intensity compared to the peaks at the edges, as shown in Fig. R1d1. **This explains why the contrast between discrete intensity peaks becomes worse for higher-order optical differentiation**.

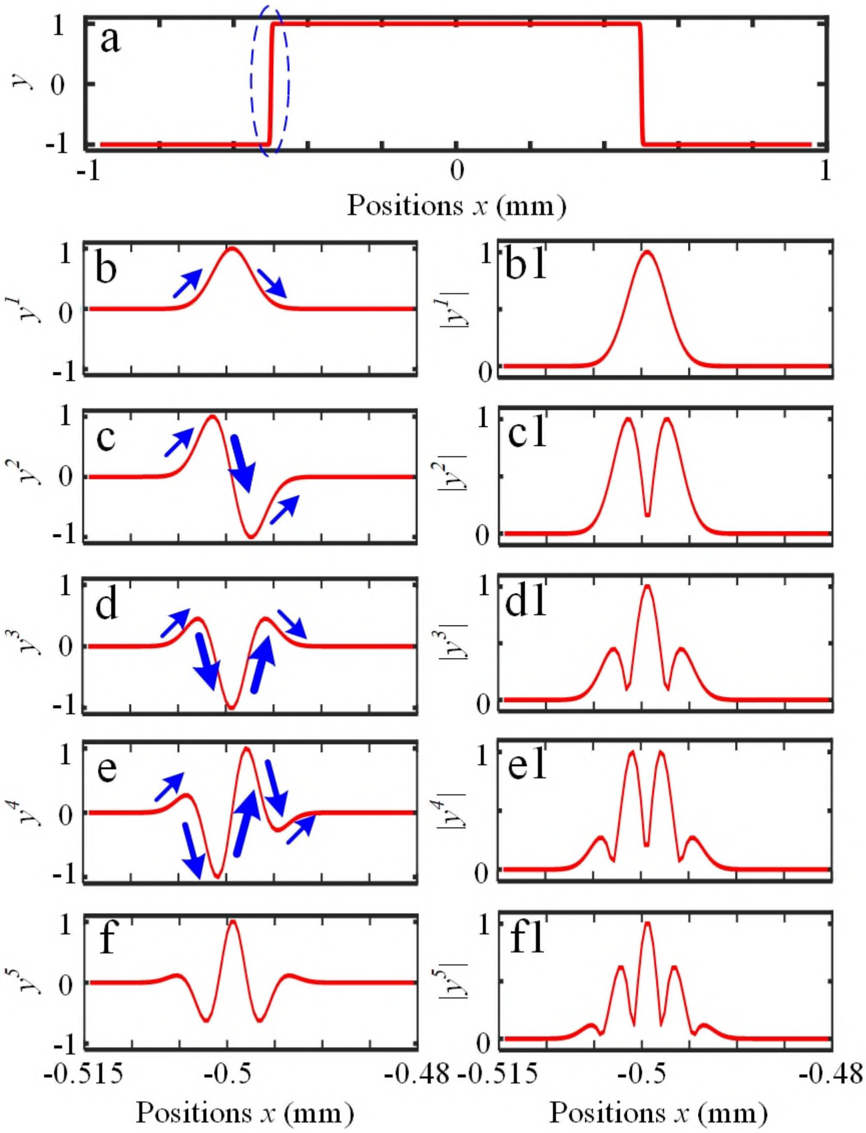

Fig. R1. High-order derivatives of the rectangular function. a corresponds to the one-dimensional rectangular function. b-f correspond to the first to fifth-order derivatives of the left edge of the rectangular function. b1-f1 represent absolute values of the corresponding high-order derivatives. Here, the direction of the blue arrow represents the direction of the gradient, and the thickness of the blue arrow represents the magnitude of the gradient.

On the other hand, for higher-order differentiation operations, the experimentally generated peaks lack perfect central symmetry, and small spikes appear near some peaks. This is primarily attributed to the non-smooth intensity distribution of the input object (seen in Fig.3n of the main text), and incomplete orthogonality between the incident and output polarizations. We have clarified this issue in our revision. (Seen on Page 13 in the main text)

"Also, similar to the Gaussian mode, the intensity of the peaks generated by the higher-order differentiation of the image decreases from the center toward the edges."..... "Note that by improving the smoothness of the input image's intensity distribution and enhancing the contrast of orthogonal polarization filtering, the imaging quality of higher-order differentiation can be further improved."

4. To highlight the novelty of this work, I suggest the authors give a comparison between this work and other works of spatial differentiation.

Response:

Good suggestion. Following the Reviewer's suggestion, In the section of Introduction, we have added a detailed description comparing our work with the current progress in higher-order differentiation research. (Seen on Page 4 in the main text)

"However, we note that most of these previous schemes have merely focused on first- and second-order differentiation. Several profound attempts have also been made to perform high-order optical analog differentiation[31,36] using an all-dielectric multilayer structure with a limited working bandwidth and a well-designed metasurface with a broad working bandwidth. Particularly, by leveraging the PB metasurface, the fourth-order differentiation operation of the angular spectrum has been realized[36]. However, how to realize scalable high-order differentiation of images and multiple-order parallel operation with a single device has not been fully explored. Meanwhile, what features might high-order differentiation lead to? These serve as the primary motivations for our present work."

5. I wonder if high-order differentiation can be achieved in two dimensions using the proposed method.

Response:

Good questions. Although we merely perform the partial derivatives along the *x*-direction, based on the coordinate equivalence and the proposed theory in Eq. (2), our proposal can be extended to realize the arbitrary order analog full derivatives, namely, perform high-order differentiation in two dimensions. Inspired by Reviewer 1 and Reviewer 4, to explain this issue, we have added a new section in Supplementary information. (Seen on Pages 7-8 in the Supplementary information)

"Supplementary Note 5. High-order differentiation in two dimensions.

Although we merely perform the partial derivatives along the *x*-direction, based on the coordinate equivalence and the proposed theory in Eq. (2), our proposal can be extended to realize the arbitrary order analog full derivatives, namely, perform high-order differentiation in two dimensions. Based on the concept of high-order differentiation, the higher-order derivatives of a bivariate function $f(x,y)$ can be expressed as $\frac{\partial^n f}{(\partial x^j \partial y^{n-j})}$, with $0 \le j \le n$. To realize its optical analog operation, one needs to construct a complex amplitude filter, $(ik_x)^j(ik_y)^{n-j}$, in Fourier space. Actually, the design in the main text can be directly used for partial derivatives along the *y*-direction via rotating the device 90 degrees, namely, converting the phase gradient along the y-direction. Since the variables *x* and *y* are independent, we only need to multiply the phase gradients in both directions to construct the required complex filter. Here, we use $n = 3$ as an example for illustration, and all components of third-order derivatives include, $\frac{\partial^3 f}{(\partial x^3)}$, $\frac{\partial^3 f}{(\partial x^2 \partial y^1)}$, $\frac{\partial^3 f}{(\partial x^1 \partial y^2)}$, and $\frac{\partial^3 f}{(\partial y^3)}$. The corresponding required gradient phases ϕ are $c_3 k_x^3$, $c_2 k_x^2 c_1 k_y^1$, $c_1 k_x^1 c_2 k_y^2$, and $c_3 k_y^3$, respectively, where the value of c_{1-3} is the same as those in the main text, and (k_x, k_y) is the coordinate in the Fourier plane. In other words, it denotes the position on the metasurface. Based on the principle of the PB phase, we simply arrange the orientation angle of the unit cell of the metasurface as $\frac{\phi}{2}$. As shown in the top row of Supplementary Fig. 5, we illustrated the designed gradient phase for realizing the full third-order derivatives. Then, we use a Gaussian beam as input to characterize the performance of high-order differentiation in two dimensions. The corresponding results are illustrated in the bottom row of Supplementary Fig. 5. These patterns are consistent with the theoretical model $\frac{\partial^n G(x,y)}{(\partial x^j \partial y^{n-j})} \propto G(x,y) H_j\left(\frac{x}{\sqrt{2\sigma^2}}\right) H_{n-j}\left(\frac{y}{\sqrt{2\sigma^2}}\right)$, thereby, indicating that our proposal can be extended to perform high-order differentiation in two dimensions.

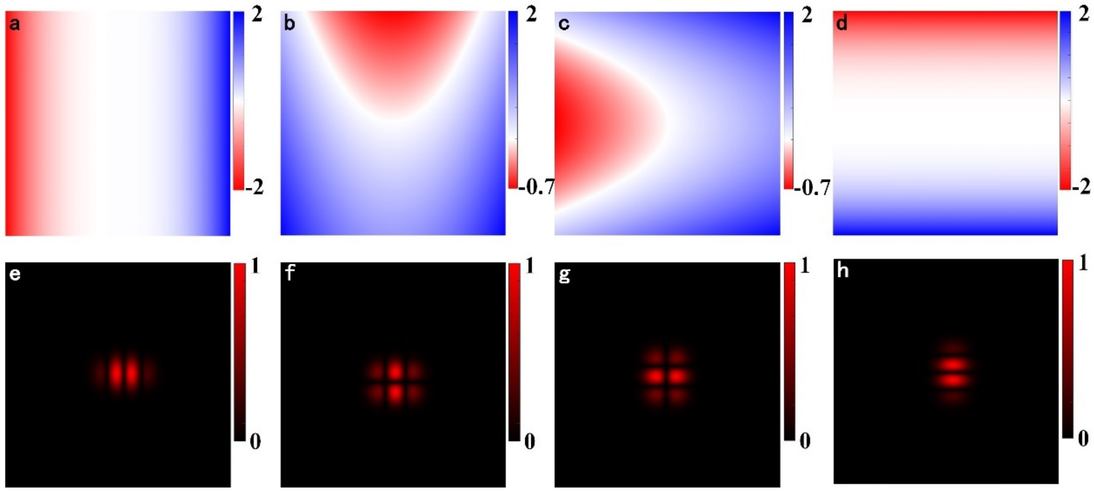

Supplementary Fig. 5. High-order differentiation in two dimensions. a-d correspond to the gradient phase of the PB metasurface for realizing the high-order differentiation $\frac{\partial^3 f}{(\partial x^3)}$, $\frac{\partial^3 f}{(\partial x^2 \partial y^1)}$, $\frac{\partial^3 f}{(\partial x^1 \partial y^2)}$, and $\frac{\partial^3 f}{(\partial y^3)}$, respectively. **e-h** illustrate the corresponding high-order differentiation of Gaussian input."

Reviewer 2:

General Comment:

The authors utilize a PB phase metasurface placed at the Fourier plane of a lens system to modulate the Fourier spectrums and realize differentiators of high orders. They experimentally demonstrate a 5th-order differentiator and used the method for detecting two closely spaced laser sources as an example of its potential applications. Several issues for the authors to check:

Response:

We thank Reviewer for the insightful and constructive comments. Following the suggestions, we have made our effort to revise the manuscript. The main changes include:

1) In Abstract and Introduction, we have clearly articulated the novelty while acknowledging the contributions and efforts of the researchers in this field;
2) In Discussion, we have added a new experiment, achieving a lateral resolution of 200 nm, to illustrate the potential of our approach in achieving nanometer-scale lateral resolution and analyzing how to further improve the resolution;
3) In Optical super-resolution, we have added some descriptions to elaborate on what each of the five layers could be and how they are correlated to the measurement system shown in Figure 4a
4) In Supplementary information, we have added a new section to discuss the scenario of multiple unknown point sources.

By addressing the Reviewer's concerns, we indeed feel that our manuscript has been much improved and can effectively avoid confusion. We sincerely wish Reviewer could consider the manuscript for publication in Nature Communications.

Specific Comments:

1. The manuscript stated "However, most previous works primarily focused on the first- and second-order operation. A fundamental challenge remains as to how to realize the high-order operation" (line 19 to 21), and it derives a universal formula,

t(k_x,k_y)=(ik_x)^n (ik_y)^m. However, such high-order differentiator has already been fully studied and reported before, for example, in Nat. Commun. (2024) 15:2237, and a universal formula has been reported for arbitrary-order differentiators and their combinations, namely, t(x,y)=∑_(j=1)^l▒[C_j (-ix)^(m_j) (-iy)^(n_j)] , in which x is the coordinate at the Fourier plane, equivalent to kx in the formula presented in the manuscript. The Nat. Commun. 2024 paper also demonstrated a fourth-order differentiator in theory and simulation and used the same 4f system and Si metasurface. The novelty of the work needs to be clarified, and the claim needs to be reconsidered.

Response:

We thank Reviewer for this insightful comment and for introducing this relevant reference [Nature Communications 15, 2237 (2024)]. This reference focuses on differential operations in k-space, presenting a novel perspective for analyzing image feature information. We agree well with Reviewer that a universal formula for high-order differentiator has been fully studied. Theoretically, based on the differentiation property of the Fourier transform, in order to perform arbitrary order differentiation operation, $\frac{\partial^{n+m}}{\partial x^n \partial y^m}$, on an input image, one needs to modulate the optical transfer function as, $t(k_x, k_y) = (ik_x)^n (ik_y)^m$, in Fourier space. Also, as indicated in the reference introduced by Reviewer, in order to realize the angular spectrum differentiation, one needs to construct a real-space transfer function $t(x,y) = \sum_{j=1}^{l} \left[C_j (-ix)^{m_j} (-iy)^{n_j} \right]$.

A critical issue is how to construct such an optical transfer function in a practical experimental system to achieve the desired differential operation, which still has aspects worth exploring. For example, by leveraging the angular-dependent transmission of an all-dielectric multilayer structure, one can construct the aforementioned transfer function [Nature Communications 13, 7944 (2022)], whereas this approach limits the broadband operation and multi-order parallel processing. Fortunately, the PB phase metasurface provides a potential solution. As shown in the reference [Nature Communications 15, 2237 (2024)] introduced by Reviewer, the authors presented an ingenious strategy for constructing the transfer function, thereby experimentally realizing second-order differentiation and theoretically demonstrating fourth-order differentiation in k-space, which is a profound progress and offers significant inspiration for implementing high-order differentiation of images in real space. Additionally, the applications of optical differentiation hold considerable room for further exploration.

In our manuscript, we leverage the PB phase to propose another different phase design approach to achieve the desired transfer function for realizing the higher-order differentiation of images in real-space. Particularly, we explored the potential applications of differential operations in optical super-resolution, which has not been explored to the best of our knowledge. Specifically, we illuminate the PB metasurface with a horizontally polarized light, $A(k)$, then we select the vertical component, i.e., LCP-RCP, from the output light field. Accordingly, the light field at the Fourier plane can be equivalently expressed as, $E = [exp(i\phi_n(k)) - exp(-i\phi_n(k))]A(k) \propto sin\big(\phi_n(k)\big)A(k)$. By leveraging the basic principle of Taylor's expansion, if $\phi_n(k)$ is a small value, the light field at the Fourier plane can be simplified as, $E \propto \phi_n(k)A(k)$. In our experiment, we select the $c_1 = 1.04 \times 10^3 m^{-1}, c_2 = 2.2 \times 10^6 m^{-1}, c_3 = 4.66 \times 10^9 m^{-1}$, $c_4 = 9.55 \times 10^{12} m^{-1}$, $c_5 = 2.03 \times 10^{16} m^{-1}$, and thereby, the approximation $sin\big(\phi_n(k)\big) = sin(c_n k^n) \approx c_n k^n$ holds true within regions indicated by dashed lines in Fig. 1 in the main text. Namely, the differentiation operation can work in these regions. Also, the working regions can be tuned by adjusting the value of c_n to meet different applications. Thanks to the careful design, we successfully implemented a record fifth-order differentiation operation in the experiment, demonstrating the excellent scalability of the proposed scheme. Meanwhile, we realized a multi-order parallel operation with a single device by leveraging angle multiplexing. Following Reviewer's suggestions, we have modified some statements to reflect our work accurately while acknowledging the contributions and efforts of the researchers in this field.

In the section of Abstract (Seen on Page 1 in the main text)

"Most previous works focused on the first- and second-order operations, while several significant works have also achieved higher-order differentiation in both real space and k-space. However, how to construct the desired optical transfer function in a practical system to realize scalable and multi-order-parallel high-order differentiation of images in real space, and particularly how to leverage it to tackle practical problems, have not been fully explored."

In the section of Introduction (Seen on Page 4 in the main text)

"However, we note that most of these previous schemes have merely focused on first- and second-order differentiation. Several profound attempts have also been made to perform high-order optical analog differentiation[31,36] using an all-dielectric multilayer structure and a well-designed metasurface. Particularly, by leveraging the PB metasurface, the fourth-order differentiation operation of the angular spectrum has been realized[36]. However, how to realize scalable high-order differentiation of images and multiple-order parallel operation with a single device has not been fully explored. Meanwhile, what features might high-order differentiation lead to? These serve as the primary motivations for our present work."

In the section of Principle (Seen on Page 5 in the main text)

"In order to perform arbitrary order differentiation operation, $\frac{\partial^{n+m}}{\partial x^n \partial y^m}$, on an input image, one merely needs to modulate the optical transfer function as, $t(k_x, k_y) = (ik_x)^n (ik_y)^m$, which has also been presented in some previous works[31,36]. In this regard, how to construct such an optical transfer function for image differentiation in a practical experimental system is critical and urgent."

2. The reported work achieved a 5um lateral resolution at NA=0.001 and stated that it is two orders of magnitude improvement over conventional method in photolithography. The alignment accuracy of photolithography machine can easily achieve tens of nm resolution and even single digit resolution for the advanced tool, far better than 5um. The authors postulate the method discussed could achieve nm

scale resolution if a high NA imaging system is used. It is recommended the author show such a high NA system to support the claim, as this is one of the key applications of this technology and the situation in high NA is very different from very small NA.

Response:

We thank Reviewer for the constructive comment. It's correct for Reviewer to point out that "*The alignment accuracy of photolithography machine can easily achieve tens of nm resolution and even single digit resolution for the advanced tool, far better than 5um.*" Actually, our intention is to express that this proposal, which surpasses the diffraction limit, has potential applications in optical alignment for lithography. We have rewritten the relevant statements to reflect our intentions better and avoid confusion.

Generally, the alignment accuracy needs to reach the sub-micron or even nanometer scale to meet the demands of different lithography applications. Following Reviewer's suggestion, over the past few weeks, we have conducted an additional experiment to demonstrate the potential of our approach in achieving nanometer-scale lateral resolution. In our demonstration, we reduced the beam waist of the Gaussian beam from 230 μm to approximately 70 μm, effectively increasing the NA from 0.0012 to 0.0038. Based on this, we verified that the high-order differentiation approach can still resolve it even with a lateral offset of 200 nm. The corresponding results are shown in Fig. R2. Actually, the resolution is primarily limited by power fluctuations, as seen from the histograms of multiple measurements for 0 nm, 200 nm, 400 nm, 600 nm, and 800 nm, indicated in the top-left inset of Fig. R2. Wherein the average intensity is resolvable, however, their power histograms overlap in some regions.

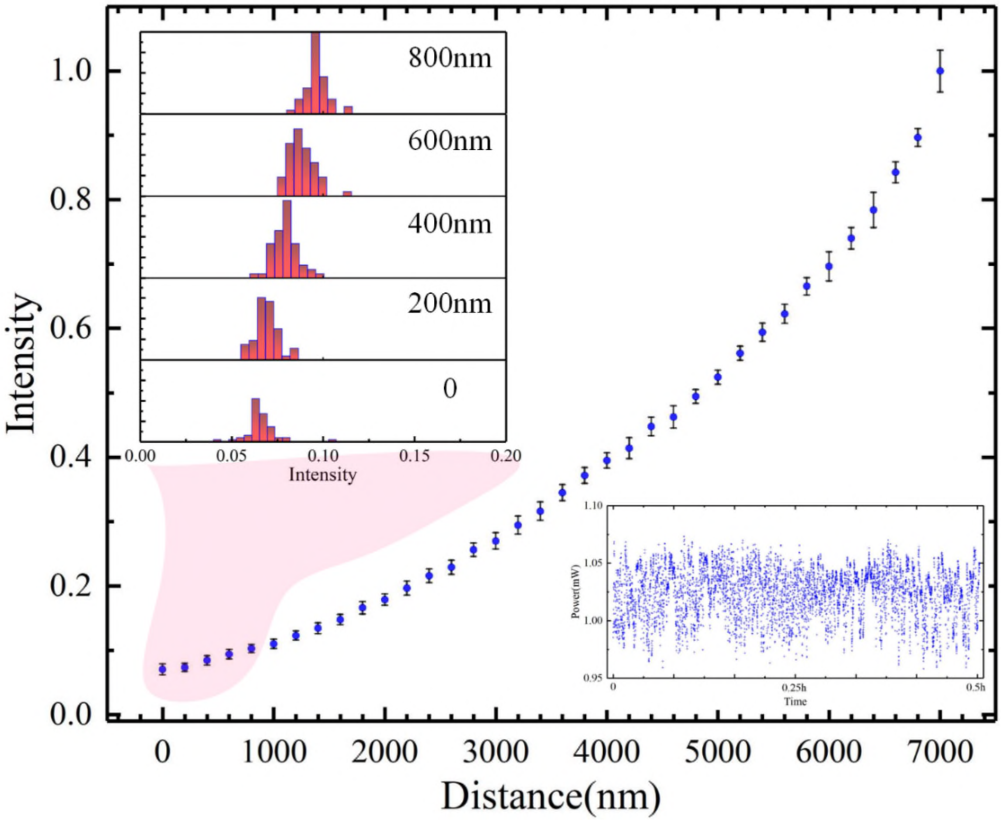

Fig. R2. Experimental demonstration of sub-micron scale optical super-resolution. Top-left inset presents the histograms of multiple measurements for lateral displacement of 0 nm, 200 nm, 400 nm, 600 nm, and 800 nm. The bottom-right inset presents the output intensity fluctuations of the laser source. Error bars represent the standard derivations of 50 independent measurements.

In our demonstration, power fluctuations primarily arise from the intensity fluctuations of the laser source. As shown in the bottom-right inset of Fig. R2, the intensity stability of our laser source is roughly 2%. On the other hand, the jitter during the movement of the motorized stage, the stability of the optical adjustment mirror mount, and the unstable interference caused by reflections at the optical components and the laser, also limit further improvements in precision. In this regard, by adopting a stable laser source or implementing feedback control, one can improve the intensity stability of the laser source to 0.1%–0.01% or even lower, which can significantly improve the resolution. Additionally, the resolution can be further improved by replacing the current motorized stage and mirror mount with more stable ones, and placing an optical isolator in the optical path. Furthermore, our system only requires a single-point detector with no spatial resolution capability, which could potentially simplify traditional complex systems.

The reason why *we postulate the method discussed could achieve nm scale resolution if a high NA imaging system is used* is that: with the same lateral displacement, a smaller beam spot (corresponding to a high NA) can induce more pronounced signal variations, enabling the resolution of smaller lateral displacements under a given level of power fluctuations, as demonstration in Fig. R2. We also agree well with Reviewer that "*the situation in high NA is very different from very small NA.*" Actually, a beam spot of several tens of micrometers is sufficient for our proposal without requiring the extreme focusing of high-NA lenses. We sincerely apologize for the confusion and imprecise descriptions in the manuscript that may have misled Reviewer. Following Reviewer's suggestions, we have modified some statements to reflect our work accurately.

In section of High-order differentiation enabled optical super-resolution: Towards optical alignment in nano-fabrication (See on Page 20 in the main text)

"Our approach, far surpassing the Rayleigh diffraction limit, provides a potential solution for optical alignment. Additionally, compared with the conventional microscopy imaging system, the proposed scheme requires only a single-point detector, which could simplify the optical system."

In section of Discussion, we have added new experiments, with the results presented in Fig. 5 (i.e., Fig. R2), and have also conducted the corresponding discussion. (See on Pages 20-21 in the main text)

"As well known, to meet the demands of different lithography applications, the alignment accuracy needs to reach the sub-micron or even nanometer scale. In our proposal, the resolution can be further improved by decreasing the size of the Gaussian beam, corresponding to an increase in the value of NA. For demonstration, we reduced the beam waist of the Gaussian beam from 230 μm to approximately 70 μm, effectively increasing the NA from 0.0012 to 0.0038. Based on this, as shown in Fig. 5, we verify that the high-order differentiation detector can still resolve it even with a lateral offset of 200 nm. Actually, the resolution is primarily limited by power fluctuations, as seen from the histograms of multiple measurements for 0 nm, 200 nm, 400 nm, 600 nm, and 800 nm, indicated in the top-left inset of Fig. 5. Wherein the average intensity is resolvable, however, their power histograms overlap in some regions. In our demonstration, power fluctuations primarily arise from the intensity fluctuations of the laser source. As shown in the bottom-right inset of Fig. 5, the intensity stability of our laser source is roughly 2%. On the other hand, the jitter during the movement of the motorized stage, the stability of the optical adjustment mirror mount, and the unstable interference caused by the reflection at the optical component and the laser also limit further improvements in precision. In this regard, the resolution can be further improved by replacing the current laser source, motorized stage, and mirror mount with more stable ones, and placing an optical isolator in the optical path. This paves the way for super-resolution microscopy imaging and for surpassing the diffraction limit in optical alignment for multiple-exposure semiconductor technologies."

3. It is claimed that two independent lasers are treated as incoherent, however, formulars (5)-(7) are derived on and only valid for two coherent light sources. Please explain.

Response:

Good questions. It's correct for Reviewer to point out that *formulas (5)-(7) are derived on and only valid for two coherent light sources*. Actually, in our demonstration, two independent laser sources are both coherent laser sources. However, since the two lasers are independent, meaning their phases are not synchronized, thereby there is no interference between them. Namely, they are incoherent with respect to each other. In this regard, the signal detected by the power meter can be expressed as,

$$P = P_1 + P_2 \propto \left| exp\left(-\frac{d_1^2}{4\sigma_1^2}\right) H_n\left(-\frac{d_1}{2\sigma_1}\right) \right|^2 + \left| exp\left(-\frac{d_2^2}{4\sigma_2^2}\right) H_n\left(-\frac{d_2}{2\sigma_2}\right) \right|^2, \quad \text{(R1)}$$

the superscripts 1 and 2 represent the two laser sources, respectively. In our manuscript, one of the lasers, i.e., laser 1, is firstly aligned with the metasurface, which leads to P_1=0. Thus, we obtain the formula (8). In this regard, these formulas exactly correspond to our actual experimental situation. If two laser sources are coherent with each other, the signal should be expressed as,

$$P = P_1 + P_2 \propto \left| exp\left(-\frac{d_1^2}{4\sigma_1^2}\right) H_n\left(-\frac{d_1}{2\sigma_1}\right) + exp\left(-\frac{d_2^2}{4\sigma_2^2}\right) H_n\left(-\frac{d_2}{2\sigma_2}\right) \right|^2, \qquad \text{(R2)}$$

We have clarified this point in our revision. (See on Page 15 in the main text)

"Note that, here, two independent laser sources are both coherent. However, since the two lasers are independent, meaning their phases are not synchronized, and thus there is no interference between them. Namely, they are incoherent with respect to each other."

Particularly, inspired by this comment and the comment 6, we have added a new section in Supplementary information to discuss the scenario of completely incoherent light and multiple unknown point sources, as shown in the response to comment 6.

4. In Figure 4b, even at d=0, there is already measurable value of 1st and 3rd order differentiators. Please explain it.

Response:

Good questions. In theory, there should be no signal at d=0. Environmental stray light is the main reason why there is still a measurable value. Due to the extremely weak signal being near zero, the influence of environmental stray light becomes noticeable. In real applications, a common method is background subtraction. Additionally, in our proposal, the implementation of higher-order differentiation relies on orthogonal polarization filtering. Consequently, imperfections in the polarization extinction ratio of the polarizer and small shifts in the polarizer's angle may introduce some noise. We have explained the sources of noise in the revision. (Seen on Page 19 in the main text)

"Note that, due to the influence of stray light in the realistic environment, imperfections in the polarization extinction ratio of the polarizer, and small shifts in the polarizer's angle, a measurable value still exists at d=0."

5. For Figure 4c, please elaborate what each of the 5 layers could be and how they are correlated to the measurement system showed in Figure 4a. In real application,

considering the substrate could be non-transparent (e.g. Si) or with other existing patterns and with large thickness, a reflective optical system is more practical.

Response:

We thank Reviewer for this constructive comment. Following Reviewer's suggestions, we have added descriptions to elaborate on what each of the five layers could be and how they are correlated to the measurement system. We also agree with Reviewer that a reflective optical system is more practical in some cases, and we have added an additional note to clarify this point. (Seen on Pages 19-20 in the main text),

"In modern semiconductor fabrication, multiple exposure techniques are often used to achieve higher processing precision or to create 3D chip configurations. During the multiple exposure process, except for the first exposure, all subsequent layers must align the mask with the patterns left by the previous mask to ensure accurate overlay. As shown in Fig. 4a, if we consider the metasurface device as a reference and the moving laser beam as a result of mask displacement, the lateral offset of the mask relative to the reference marker can be determined by monitoring the intensity output of the power meter. In this regard, the presented super-resolution detector could provide a potential solution for optical alignment. As shown in Fig. 4c, we present a proposal for optical alignment for multiple-exposure semiconductor manufacturing systems. Our proposal involves embedding a high-order differentiator metasurface directly into the semiconductor chips being produced, and integrating a linear grating on the mask, which is used to guide the transmitted or reflected light. Alternatively, a coating can also be applied to replace the grating to allow only the grating area to transmit or reflect light. Then, illuminating the first mask with a laser beam, the lateral displacement of the transmitted light spot relative to the metasurface will change as the mask moves. According to the concept presented in Fig. 4a, we can determine this lateral displacement by monitoring the intensity output of the power meter. After completing the exposure of the first layer, we repeat the above steps to align and expose the other masks. This proposal could also find potential applications in the field of 3D chip-stacking and heterogeneous integration. In this consideration, the five layers in Fig. 4c can be seen as the chips to be stacked. Note that, for simplicity, we only present the transmission case in Fig. 4c. Whereas, in some certain applications, considering the substrate could be non-transparent or with a large thickness, a reflective optical system is more practical. In this regard, our approach, far surpassing the Rayleigh diffraction limit, provides a potential solution for optical alignment. Additionally, compared with the conventional microscopy imaging system, the proposed scheme requires only a single-point detector, which could simplify the optical system."

6. The current super-resolution experiment is based on two lasers with already known and fixed intensity and beam waists. In real situation, the intensity and number of point objects are un-known. How would these affect the effectiveness of the current method?

Response:

Enlightening questions. Inspired by Comment 6 and the concerns raised in Comment 3, we have added a new section in Supplementary information to discuss the scenario of completely incoherent light and multiple unknown point sources, which could have potential applications in super-resolution fluorescence microscopy. (Seen on Pages 9-12 in the Supplementary information)

"Supplementary Note 6. Optical super-resolution with unknown incoherent and coherent illumination.

In the main text, we use two independent laser sources for optical alignment, which are incoherent with respect to each other. Note that the intensity and number of the lasers are known in advance. In some practical applications, the intensity and number of point sources may be unknown, and the light source could be incoherent, such as incoherent imaging and fluorescence microscopy. To simplify, here, we take the one-dimensional case as an illustrative example. Assume that there are n unknown point sources distributed along the x-axis, and their positions can be expressed as d_i. For each point source, after passing through the metasurface, the resultant incoherent light can be expressed as,

$$E_{i,m} = A_i c_m G(x-d_i) H_m\left(\frac{x-d_i}{\sqrt{2}\sigma}\right), \tag{S1}$$

where $G(x-d_i)$ is the Gaussian function, which is exactly the transfer function of a point source, as indicated in the main text, and A_i is the amplitude of point source *i*, *m* is the order of Hermite polynomial and also corresponds to the order of differentiation, and c_m is the constant coefficient of *m*-order differentiation. Being different from the coherent illumination, in order to acquire the component of fundamental mode with incoherent source, we routinely need to perform ensemble averaging[1], namely,

$$P_{i,m} = \iint \langle E_{i,m}(x_1) G(x_1) E^*_{i,m}(x_2) G(x_2)\rangle \, d_{x_1} d_{x_2}. \tag{S2}$$

According to the property of incoherent, namely,

$$\langle E_{i,m}(x_1) G(x_1) E^*_{i,m}(x_2) G(x_2)\rangle = \left|E_{i,m}(x_1) G(x_1)\right|^2 \times \delta(x_1 - x_2). \tag{S3}$$

In this regard, Eq. (S2) can be expressed as,

$$P_{i,m} = I_i \left|c_m\right|^2 \int \left|G(x-d_i) H_m\left(\frac{x-d_i}{\sqrt{2}\sigma}\right)\right|^2 \left|G(x)\right|^2 dx, \tag{S4}$$

which is exactly similar to the incoherent imaging system in Fourier optics[2]. By leveraging the integral formula,

$$\int_{-\infty}^{\infty} exp[-(x-y)^2]\, H_m(\alpha x) H_n(\alpha x) dx$$
$$= \pi^{\frac{1}{2}} \sum_{k=0}^{min(m,n)} 2^k k! \binom{m}{k}\binom{n}{k} (1-\alpha^2)^{\frac{m+n}{2}-k} H_{m+n-2k}\left[\frac{\alpha y}{(1-\alpha^2)^{\frac{1}{2}}}\right], \tag{S5}$$

we conclude that,

$$P_{i,m} \propto I_i \sum_{k=0}^{m} 2^k k! \binom{m}{k}\binom{m}{k} (1-\alpha^2)^{m-k} exp\left(-\frac{d_i^2}{2\sigma^2}\right) H_{2m-2k}\left[\frac{-\sqrt{6} d_i}{6\sigma}\right]. \tag{S6}$$

Considering all unknown point sources, for *m*-order differentiation, the total signal can be expressed as,

$$P_m = \sum_{i=1}^{n} P_{i,m}. \tag{S7}$$

After performing a series of high-order differentiation operations, the positions and intensities of the unknown point sources are embedded in the coefficients of the Hermite polynomials, which subsequently influence the intensity of P_m. It is similar to computational ghost imaging[3], where a series of spot patterns with specific spatial distributions, such as Laguerre-Gaussian modes, Hermite-Gaussian modes, and Hadamard orthogonal matrices, are successively used to illuminate the object. The transmitted or reflected light intensity from the object is then detected by a bucket detector. This intensity corresponds to the coefficients of the corresponding modes, which are subsequently processed to recover the information of the object under test. Accordingly, based on Eq. (6) and Eq. (7), the positions and intensities of the unknown point sources can be estimated. However, it's hard to obtain a clear analytical expression. Some advanced inverse solving algorithms or neural networks can be used to tackle this issue.

If the light source is coherent, namely, these unknown point sources are coherent with each other, such as the coherent imaging, this problem is exactly consistent with the computational ghost imaging or state tomography. Specifically, based on the Eq. (8) in the main text, for each point source and a certain differentiation operation, the signal induced by the proposed super-resolution device can be expressed as,

$$B_{i,m} \propto A_i\, exp(i\varphi_i)\, exp\left(-\frac{d_i^2}{4\sigma^2}\right) H_m\left(-\frac{d_i}{2\sigma}\right), \tag{S8}$$

where $A_i\, exp(i\varphi_i)$ represents the complex amplitude of the point source *i*. Considering all unknown point sources, for *m*-order differentiation, the total signal can be expressed as,

$$B_m \propto \sum_{i=1}^{n} B_{i,m}. \tag{S9}$$

If we consider the unknown point sources as a continuously varying image or wavefunction $f(x)$, Eq. (S9) can be expressed as,

$$B_m \propto \int A_i\, exp(i\varphi_i)\, exp\left(-\frac{d_i^2}{4\sigma^2}\right) H_m\left(-\frac{d_i}{2\sigma}\right) d(d_i). \tag{S10}$$

The above overlap integral is exactly consistent with the mode filtering in structured light[4]. If we acquire the value of B_m, the distribution of the unknown point sources can be revealed by,

$$f(x) = \sum_m B_m\, exp\left(-\frac{x^2}{4\sigma^2}\right) H_m\left(-\frac{x}{2\sigma}\right). \tag{S11}$$

Actually, B_m is a complex value. However, in the experiment, the power meter can merely acquire the intensity information, namely, $|B_m|^2$. In order to acquire the phase information of B_m, similar to the polarization state reconstruction and state tomography[5], it is necessary to introduce the superposition detection of different-order differentiations. The above theory of coherent and incoherent illumination could have potential applications in super-resolution imaging, and we leave these possibilities in our future studies."

The corresponding descriptions have also been added to the main text. (Seen on Page 22)

"Additionally, as discussed in Supplementary Note 6, the proposed scheme for optical super-resolution could be extended to resolve multiple unknown point light sources, which has potential applications in super-resolution imaging."

7. What is the reason to have PMMA baked for 1 hour, which is much longer than the conventional practice of just several minutes? Why K9 glass is chose as the substrate?

Response:

We are grateful for Reviewer's thorough review. In our lab, we have consistently followed a relatively long (1-hour) baking process to ensure the stable formation of the PMMA layer. Sometimes, in a rush, some colleagues have also tried a 15-minute baking process, and the fabricated samples also work well. We appreciate Reviewer's guidance in expediting our sample processing workflow. In future research, we will try to modify the recipe to shorten the baking time and evaluate how it works. As for the K9 glass, we chose it as the substrate due to its excellent mechanical properties, including high intensity, high hardness, and high heat resistance, which help reduce the risk of sample damage. We have added corresponding descriptions in our revision to clarify these points. (Seen on Page 23 in the main text)

"Subsequently, an 80 nm PMMA layer is spin-coated and baked at 180°C for 1 hour. Our lab has consistently followed this baking process, as it yields stable results...... Note that we use K9 glass as the substrate due to its excellent mechanical properties, including high strength, hardness, and heat resistance, which reduce the risk of sample damage."

Reviewer 3:

General Comment:

I co-reviewed this manuscript with one of the reviewers who provided the listed reports. This is part of the Nature Communications initiative to facilitate training in peer review and to provide appropriate recognition for Early Career Researchers who co-review manuscripts.

Response:

We thank Reviewer for the co-review. The three sets of review comments are all constructive and enlightening. After addressing all Reviewers' concerns, our manuscript has been much improved, and we sincerely wish Reviewer could consider the manuscript for publication in Nature Communications.

Reviewer 4:

General Comment:

This manuscript proposes a high-dimensional differentiation (i.e., "cascaded" edge detection) of optical images using a Si metasurface multiplexed to provide different orders through different diffraction channels. It claims an experimental demonstration of all-optical differentiations up to the fifth order based on a simple intensity object and a phase object. Pancharatnam-Berry phase allows for broadband operation. More interesting aspect of the paper is the potential utilization of differentiation to detect short separations between two objects beyond the Rayleigh limit. With this approach they can detect a separation of 5 um, which is comparable to the pixel size.

For this paper to be published in Nature Communications, the authors should better highlight the novelty and the limits of their technique.

Response:

We thank Reviewer for the positive recommendations and the constructive comments. Following these suggestions, we have tried our best to rephrase our work to highlight the novelty and the limits of our scheme accurately. The main changes include:

1) In Introduction, we have clearly articulated the novelty while acknowledging the contributions and efforts of the researchers in this field;
2) In Principle, we have rewritten and articulated the design strategy;
3) In Supplementary information, we have added four new sections to discuss the limits of our scheme, High-order differentiation in two dimensions, combining the functions of lenses with the metasurface, and High-order differentiation operation on phase image, respectively.

By addressing Reviewer's concerns, we indeed feel that the manuscript has been much improved, and we sincerely wish Reviewer could consider the manuscript for publication in Nature Communications.

Specific Comments:

1. It's been mentioned that all-dielectric multilayer structures are used for high-order

differentiation, but the present manuscript argues a general design strategy. Although mathematical form of high-order differentiation is given (unfortunately with some confusion), the design strategy is not well described for metasurfaces for an arbitrary order. Also, the manuscript only investigates 1D filtering. There is an error or confusion in the manuscript as for how an arbitrary order differentiation is defined even mathematically. The partial derivatives on the left hand side of Eq. 2 is not equal to the one given in the next line after Eq. 2.

Response:

We thank Reviewer for these constructive comments. We sincerely apologize for not providing a clear explanation in the manuscript, which caused confusion for Reviewer. Theoretically, based on the differentiation property of Fourier transform, in order to perform arbitrary order differentiation operation, $\frac{\partial^{n+m}}{\partial x^n \partial y^m}$, on an input image, one needs to modulate the optical transfer function as, $t(k_x, k_y) = (ik_x)^n (ik_y)^m$, in Fourier space, which has also indicated in some related reference, such as in [Nature Communications 13, 7944 (2022)].

A critical issue is how to construct such an optical transfer function in a practical experimental system to achieve the desired differential operation, which still has many aspects worth exploring. For example, by leveraging the angular-dependent transmission of all-dielectric multilayer structure, one can construct the aforementioned transfer function [Nature Communications 13, 7944 (2022)], whereas this approach limits the broadband operation and multi-order parallel processing. In our manuscript, we leverage the PB phase to propose another different and scalable phase design approach to achieve the desired transfer function for realizing the higher-order differentiation of images in real-space. Particularly, we explored the potential applications of differential operations in optical super-resolution, which has not been explored to the best of our knowledge. Thanks to the careful design, we successfully implemented a record fifth-order differentiation operation in the experiment, demonstrating the excellent scalability of the proposed scheme. Meanwhile, we realized a multi-order parallel operation with a single device by leveraging angle multiplexing. Following Reviewer's suggestions, we have clarified the novelty and design strategy in our revision.

In the section of Abstract, we have modified some statements to reflect our work accurately while acknowledging the contributions and efforts of the researchers in this field. (Seen on Page 4 in the main text)

"Most previous works focused on the first- and second-order operations, while several significant works have also achieved higher-order differentiation in both real space and k-space. However, how to construct the desired optical transfer function in a practical system to realize scalable and multi-order-parallel high-order differentiation of images in real space, and particularly how to leverage it to tackle practical problems, have not been fully explored."

In the section of Principle of high-order optical differentiation with PB metasurface, we have rewritten Eq. (2) to avoid confusion and have also clarified the design strategy. (Seen on Pages 5-7 in the main text)

"Drawing on the differentiation property of the Fourier transform,

$$\frac{\partial^{n+m} E_{in}(x,y)}{\partial x^n \partial y^m} = \mathcal{F}^{-1}\left[(ik_x)^n (ik_y)^m \mathcal{F}\left(E_{in}(x,y)\right)\right], \quad (2)$$

accordingly, in order to perform arbitrary order differentiation operation, $\frac{\partial^{n+m}}{\partial x^n \partial y^m}$, on an input image $E_{in}(x,y)$, one merely needs to modulate the optical transfer function as, $t(k_x, k_y) = (ik_x)^n (ik_y)^m$, which has also been presented in some previous works[31,36]. In this regard, how to construct such an optical transfer function for image differentiation in a practical experimental system is critical and urgent. Whereas, achieving the desired optical transfer function, namely conducting arbitrary intensity modulation directly with metasurfaces, remains a challenge. Due to its phase robustness and lower demands on fabrication precision, PB metasurfaces with polarization-assisted phase modulation present a promising solution. Here, leveraging the PB phase, we propose a scalable approach for constructing transfer functions to achieve high-order differentiation operations.

Without loss of generality, here, we take the partial derivative in the *x*-direction as an example. Theoretically, when the right-handed and left-handed circular polarization (RCP and LCP) light illuminate a PB metasurface, the polarization states of transmitted or reflected light switch to LCP and RCP, meanwhile acquiring additional phase $exp(-i\phi(k_x))$ and $exp(i\phi(k_x))$, respectively. This is because the unit cells of PB metasurfaces can be seen as half-wave plates (HWP) with an orientation angle, $\frac{\phi(k_x)}{2}$. In this regard, if the PB metasurface is placed at the Fourier plane of a 4f imaging system, and the input image has a horizontal polarization state, we select the vertical polarization component after it passes through the metasurface. Accordingly, the light field behind the metasurface can be expressed as,

$$\begin{aligned} E_F &= \left[\exp(i\phi(k_x)) - \exp(-i\phi(k_x))\right] A(k_x) \\ &= 2i\sin\left(\phi(k_x)\right) A(k_x). \end{aligned} \quad (3)$$

If we design the metasurface to enable $sin\left(\phi(k_x)\right) \propto (ik_x)^n$, we can thereby construct the desired optical transfer function to achieve high-order differentiation operations. Drawing on the basic principle of Taylor's expansion, if $\phi(k_x)$ is a small value close to zero, $sin\left(\phi(k_x)\right) \approx \phi(k_x)$. Accordingly, we artificially tailor the gradient phase of the PB metasurface as, $\phi_n(k_x) = c_n(k_x)^n$, with k_x also representing the coordinate in the plane of the metasurface and c_n being a constant to ensure that $\phi_n(k_x)$ is sufficiently small. Accordingly, Eq. (3) can be expressed as,

$$E_{\mathcal{F}} \propto (k_x)^n A(k_x), \quad (4)$$

which is formally consistent with Eq. (2).

For demonstration, here, we set $c_1 = 1.04 \times 10^3 m^{-1}$, $c_3 = 4.66 \times 10^9 m^{-1}$, and $c_5 = 2.03 \times 10^{16} m^{-1}$, for realizing first-, third-, and fifth-order differentiation operation, the corresponding phase gradients are illustrated in Fig. 1. As shown in Fig. 1a, for the particular case with $n = 1$, which is the commonly used linear gradient phase for edge detection or first-order differentiation operation[23]. As shown in Fig. 1b and Fig. 1c, we can easily prepare the required optical transfer function for realizing high-order differentiation."

Actually, our proposal can be easily extended to embrace high-order differentiation in two dimensions. As Inspired by Reviewer 1 and 4, we have added a new section in Supplementary information to clarify this issue. (Seen on Pages 7-8 in Supplementary information)

"Supplementary Note 5. High-order differentiation in two dimensions.

Although we merely perform the partial derivatives along the *x*-direction, based on the coordinate equivalence and the proposed theory in Eq. (2), our proposal can be extended to realize the arbitrary order analog full derivatives, namely, perform high-order differentiation in two dimensions. Based on the concept of high-order differentiation, the higher-order derivatives of a bivariate function $f(x,y)$ can be expressed as $\frac{\partial^n f}{(\partial x^j \partial y^{n-j})}$, with $0 \leq j \leq n$. To realize its optical analog operation, one needs to construct a complex amplitude filter, $(ik_x)^j(ik_y)^{n-j}$, in Fourier space. Actually, the design in the main text can be directly used for partial derivatives along the *y*-direction via rotating the device 90 degrees, namely, converting the phase gradient along the y-direction. Since the variables *x* and *y* are independent, we only need to multiply the phase gradients in both directions to construct the required complex filter. Here, we use $n = 3$ as an example for illustration. All components of third-order derivatives include $\frac{\partial^3 f}{(\partial x^3)}$, $\frac{\partial^3 f}{(\partial x^2 \partial y^1)}$, $\frac{\partial^3 f}{(\partial x^1 \partial y^2)}$, and $\frac{\partial^3 f}{(\partial y^3)}$. The corresponding required gradient phases ϕ are $c_3 k_x^3$, $c_2 k_x^2 c_1 k_y^1$, $c_1 k_x^1 c_2 k_y^2$, and $c_3 k_y^3$, respectively, where the value of c_{1-3} is the same as those in the main text, and (k_x, k_y) is the coordinate in the Fourier plane. In other words, it denotes the position on the metasurface. Based on the principle of the PB phase, we simply arrange the orientation angle of the unit cell of the metasurface as $\frac{\phi}{2}$. As shown in the top row of Supplementary Fig. 5, we illustrated the designed gradient phase for realizing the full third-order derivatives. Then, we use a Gaussian beam as input to characterize the performance of high-order differentiation in two dimensions. The corresponding results are illustrated in the bottom row of Supplementary Fig. 5. These patterns are consistent with the theoretical model $\frac{\partial^n G(x,y)}{(\partial x^j \partial y^{n-j})} \propto G(x,y) H_j\left(\frac{x}{\sqrt{2\sigma^2}}\right) H_{n-j}\left(\frac{y}{\sqrt{2\sigma^2}}\right)$, thereby, indicating that our proposal can be extended to perform high-order differentiation in two dimensions.

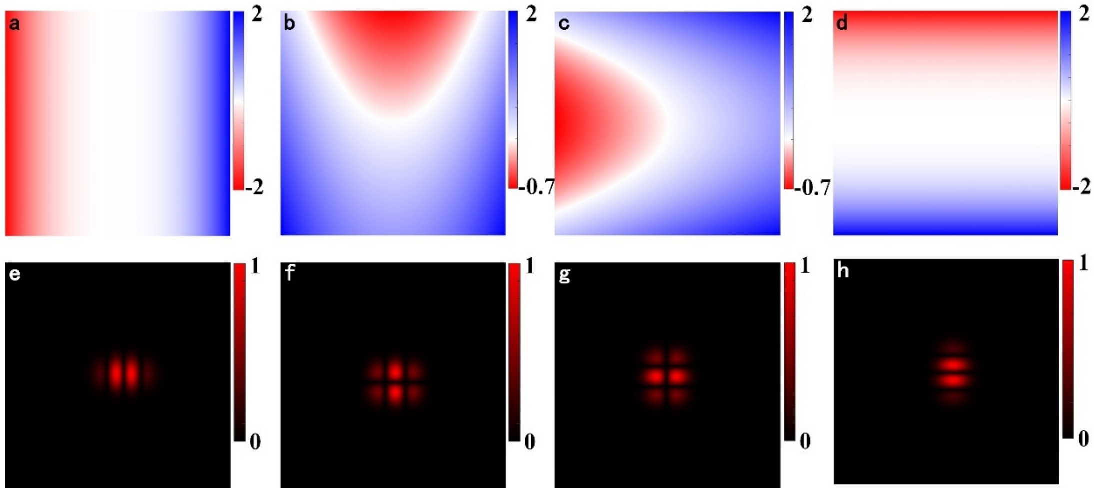

Supplementary Fig. 5. High-order differentiation in two dimensions. a-d correspond to the gradient phase of the PB metasurface for realizing the high-order differentiation $\frac{\partial^3 f}{(\partial x^3)}$, $\frac{\partial^3 f}{(\partial x^2 \partial y^1)}$, $\frac{\partial^3 f}{(\partial x^1 \partial y^2)}$, and $\frac{\partial^3 f}{(\partial y^3)}$, respectively. **e-h** illustrate the corresponding high-order differentiation of Gaussian input."

2. Also, what are the limitations of the present implementation with metasurfaces? How far can it go in terms of differentiation order? What are the theoretical and practical limitations (metasurface related, detection related, etc.)?

Response:

Good questions. As indicated in the above Response, in theory, by selecting the value of c_n, one can ensure that $E_{\mathcal{F}}$ (Eq. (3) in the main text) can be approximated as $(k_x)^n A(k_x)$ within a specific working region, thereby enabling the arbitrary order differentiation operation. In this regard, there are no limits to the differentiation order in theory. However, for most functions, as the order of differentiation increases, the signal strength typically diminishes, which places higher demands on the detector's response. Additionally, the phase gradient of the metasurface for realizing higher-order differentiation rises exponentially, requiring more precise alignment, which is also indicated in Fig. 4b. Therefore, higher alignment accuracy is essential to achieve reliable results for high-order differentiation in practical experiments. Furthermore, orthogonal polarization filtering is required in our scheme, which also reduces the intensity of the differentiation signal. In order to clarify this point, we have added a new section in Supplementary information. (Seen on Pages 5-7 in Supplementary information)

"Supplementary Note 4. The numerical simulation of high-order differentiation operation

The proposed scheme can be extended to embrace arbitrary order differentiation operation merely by setting a suitable gradient phase of the PB metasurface. Specifically, by selecting the value of c_n, one can ensure that $E_{\mathcal{F}}$ (Eq. (3) in the main text) can be approximated as $(k_x)^n A(k_x)$ within a specific working region, thereby, enabling the arbitrary order differentiation operation. Here, as a reference, we design and optimize the parameters required for the 6th to 10th-order differentiation operations. As shown in Supplementary Fig. 4, we use a Gaussian beam as the input and employ the optimized parameters c_n, to achieve its higher-order differentiation operations. The corresponding c_n required for each order are listed in the upper left corner of each figure. The parameters of the unit cell are consistent with those described in the main text. The separated lobes in Supplementary Fig. 4 are consistent with the theoretical predictions indicated by $\frac{\partial^n G(x,y)}{\partial x^n} \propto G(x,y)H_n\left(\frac{x}{\sqrt{2\sigma^2}}\right)$ (seen in the main text), which implies that our approach can be extended to higher orders. However, for most functions, as the order of differentiation increases, the signal strength typically diminishes, which places higher demands on the detector's response. Additionally, the phase gradient of the metasurface for realizing higher-order differentiation rises exponentially, requiring more precise alignment, which is also indicated in Fig. 4b in the main text. Therefore, higher alignment accuracy is essential to achieve reliable results for high-order differentiation in practical experiments. Furthermore, orthogonal polarization filtering is required in our scheme, which also reduces the intensity of the differentiation signal.

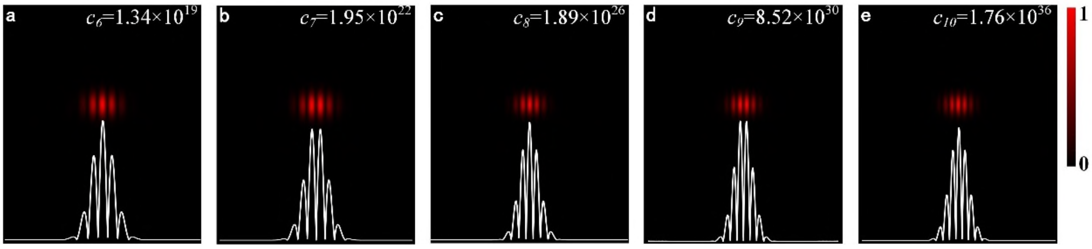

Supplementary Fig. 4. Numerical simulations for the high-order differentiation. a-e correspond to the differentiation of Gaussian input from 6th to 10th-order. The white lines therein represent the intensity distributions along the center of the red patterns. The unit m^{-1} for c_n at the top-right corner is omitted."

3. One of the important motivations of using metasurfaces is the miniaturization especially in the direction of optical axis. Is it really feasible to combine the functions of other optical components, lenses (e.g., Fourier transform, etc.) with the metasurface while preserving high-order differentiation functionality?

Response:

Enlightening questions. The answer is yes. Actually, in the previous works, some researchers have already combined the lens with the metasurfaces to realize the first-order differentiation functionality [Nanophotonics 10, 741 (2020); and Advanced Functional Materials 32, 2106050 (2022)] in the experiment. Inspired by Reviewer's questions, we have added a new section in the Supplementary information to clarify this point from both theoretical and simulation perspectives. (Seen on Pages 12-14 in the Supplementary information)

"Supplementary Note 7. The theoretical and numerical simulations of the metalens for high-order differentiation operations.

As well known, the important motivation for using metasurfaces is the miniaturization, especially in the direction of the optical axis. Here, we explore the potential of combining the phase of differentiation operation and the Fourier lens. Considering a situation where the transmission of the prepared metalens can be expressed as,

$$P \propto A(x_2, y_2)\, exp\left(-j\frac{k}{2f}(x_2^2 + y_2^2)\right)(ix_2)^n, \qquad \text{(S12)}$$

wherein the first term and second term represent the aperture and the phase of the conventional lens, respectively, and the third term represents the transfer function of the high-order differentiation. If the object $O(x_1, y_1)$ is placed at a distance of D1 in front of the metalens, and the receiving screen is positioned at a distance of D2 behind the metalens, meanwhile, D1 and D2 satisfy the thin lens equation, namely,

$$\frac{1}{D1} + \frac{1}{\mathrm{D2}} = \frac{1}{f}, \tag{S13}$$

where f is the focal length of the metalens. Thereby, based on the imaging with a single lens in Fourier optics[2], the signal at the receiving screen can be expressed as,

$$O_r(x, y) = \frac{1}{M} O\left(-\frac{x}{M}, -\frac{y}{M}\right) * \mathcal{F}\big(A(x_2, y_2)\big) * \mathcal{F}\big((ix_2)^n\big), \tag{S14}$$

where $M = \frac{D2}{\mathrm{D1}}$ represents the magnification, and * represents the convolution operation. The subscript 2 represents the coordinates on the lens plane. $O\left(-\frac{x}{M}, -\frac{y}{M}\right)$ represents an inverted image. By leveraging the formulas,

$$\delta^{(n)}(x) = \mathcal{F}[(ik)^n]$$

$$f(x) * \delta^{(n)}(x) = f^{(n)}(x), \tag{S15}$$

the signal at the receiving screen can be concluded as,

$$O_r(x, y) = \frac{\partial^n}{\partial x^n}\left[\frac{1}{M} O\left(-\frac{x}{M}, -\frac{y}{M}\right) * \mathcal{F}\big(A(x_2, y_2)\big)\right]. \tag{S16}$$

In Eq. (S16), $\mathcal{F}\big(A(x_2, y_2)\big)$ is the point spread function of the conventional lens, which can usually be approximated as a Gaussian function. This is generally encountered in lens imaging. From Eq. (S16), we can see that the high-order differentiation can also be realized by combining the lens with the metasurfaces, thus providing a potential for miniaturizing the optical system in the direction of the optical axis. Also, by using the angular spectrum propagation method, we numerically simulated the high-order differentiation effects by integrating the lens with the high-order differentiation transfer function. The numerical results are shown in Supplementary Fig. 6, which demonstrate that it is indeed feasible to integrate the functions of other optical components, such as lenses (e.g., Fourier transforms), with the metasurface while maintaining high-order differentiation functionality.

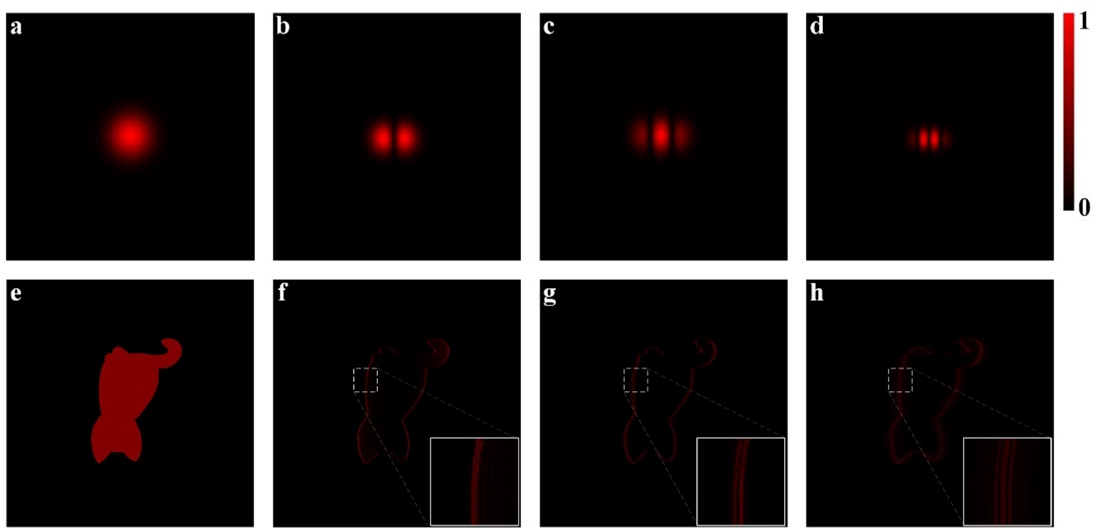

Supplementary Fig. 6. Numerical simulations for the high-order differentiation operation with the differentiation metalens. a represents the original Gaussian mode. b-d corresponds to its first-order, second-order, and third-order differentiation. e represents the input image "cat," f-h correspond to its first-order, second-order, and third-order differentiation. The insets in f-h show the magnified details."

4. Are there any other unique applications besides super-resolution detection of two point sources?

Response:

Generally, optical differentiation operation is used for the edge detection, as presented in Fig. 3 in the main text. Based on edge detection, optical differentiation operation is also used for phase reconstruction [Nature Photonics 14, 109 (2020)]. Furthermore, based on the theoretical simulation in Supplementary Note 4 and Supplementary Note 5, our scheme can be extended to embrace high-order analog full derivatives, which can be used for optical analog computing and wavefunction estimation with Taylor expansion. Also, based on the theoretical model presented in Supplementary Note 6, which is an added section (see the Response to comment 8), high-order differentiation could offer a potential solution for super-resolution imaging. Additionally, it can also be used for quantum image processing [Science Advances 6, eabc4385 (2020)]. We have presented these possibilities in the section of Discussion.

5. Given that minimum detected separation is 5 um, (i.e., already comparable to pixel size), what type of advantage would high NA system provide, without having higher resolution camera?

Response:

Good question. Compared with using the camera to capture the image of two closed point sources, which are limited by the diffraction, namely, Rayleigh limit, our scheme merely requires a bucket detector, i.e., a power meter without spatial resolution capability. By employing advanced algorithms or machine learning to analyze the spots captured by the camera, it is possible to analyze spot displacements at the level of camera pixel size. However, it would consume computational resources. In the manuscript, we can achieve a smaller detected separation for a smaller beam waist, corresponding to a larger NA, which would exceed the resolution of existing cameras (micrometer scale). In the past few weeks, we have added an additional experiment to clarify this point. In our demonstration, we reduced the beam waist of the Gaussian beam from 230 μm to approximately 70 μm, effectively increasing the NA from 0.0012 to 0.0038. Based on this, we verified that the high-order differentiation approach can still resolve it even with a lateral offset of 200 nm. The corresponding results are shown in Fig. R1.

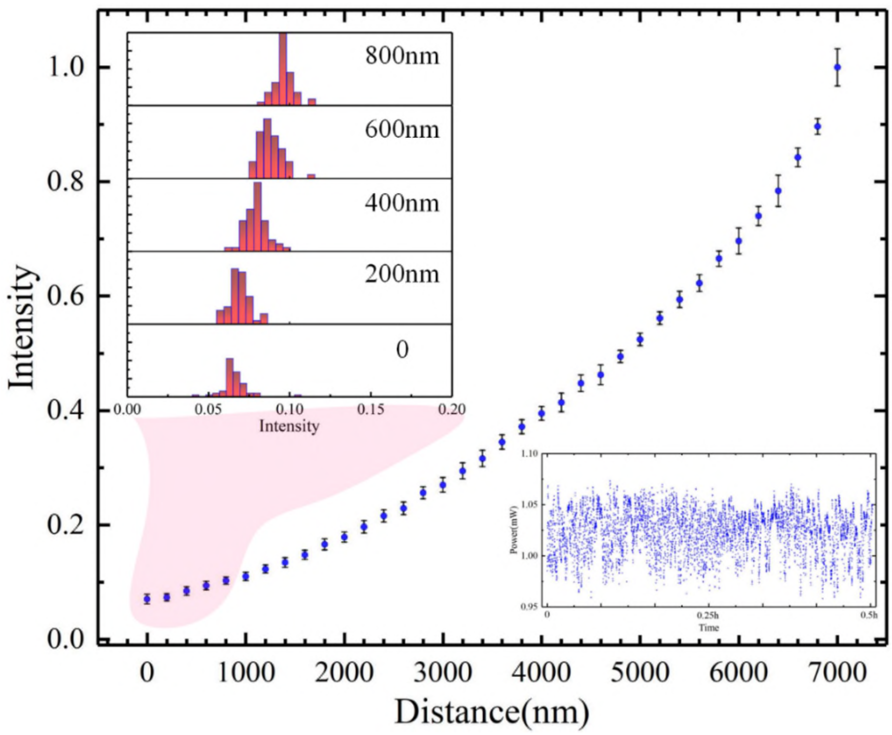

Fig. R1. Experimental demonstration of sub-micron scale optical super-resolution. Top-left inset presents the histograms of multiple measurements for lateral displacement of 0 nm, 200 nm, 400 nm, 600 nm, and 800 nm. The bottom-right inset presents the output intensity fluctuations of the laser source. Error bars represent the standard derivations of 50 independent measurements.

In section of Discussion, we have added this new experiment, with the results presented in Fig. 5 (i.e., Fig. R1), and have also conducted the corresponding discussion. (Seen in Pages 20-22 in the main text)

"As well known, to meet the demands of different lithography applications, the alignment accuracy needs to reach the sub-micron or even nanometer scale. In our proposal, the resolution can be further improved by decreasing the size of the Gaussian beam, corresponding to an increase in the value of NA. For demonstration, we reduced the beam waist of the Gaussian beam from 230 μm to approximately 70 μm, effectively increasing the NA from 0.0012 to 0.0038. Based on this, as shown in Fig. 5, we verify that the high-order differentiation detector can still resolve it even with a lateral offset of 200 nm. Actually, the resolution is primarily limited by power fluctuations, as seen from the histograms of multiple measurements for 0 nm, 200 nm, 400 nm, 600 nm, and 800 nm, indicated in the top-left inset of Fig. 5. Wherein the average intensity is resolvable, however, their power histograms overlap in some regions. In our demonstration, power fluctuations primarily arise from the intensity fluctuations of a laser source. As shown in the bottom-right inset of Fig. 5, the intensity stability of our laser source is roughly 2%. On the other hand, the jitter during the movement of the motorized stage, the stability of the optical adjustment mirror mount, and the unstable interference caused by the reflection at the optical component and the laser also limit further improvements in precision. In this regard, the resolution can be further improved by replacing the current laser source, motorized stage, and mirror mount with more stable ones, and placing an optical isolator in the optical path. This paves the way for super-resolution microscopy imaging and for surpassing the diffraction limit in optical alignment for multiple-exposure semiconductor technologies."

6. In Fig. 3h, although a phase object is used for differentiation, the main impact is not really coming from the phase distribution. The edge detection is still effective on the sharp intensity variations at the outermost boundary of the square (i.e., see the black square outline). Therefore, this figure does not really seem to demonstrate differentiation on phase distribution. What's the intensity contrast between the interior of the square and the black outline?

Response:

Enlightening comments. Theoretically, the light falling onto the phase edge of the object (corresponding to the components of high frequency) can be scattered or diffracted out of the numerical aperture of the subsequent collection optics. In our demonstration, the phase jump between the inside and outside area of the square is strictly π, such that it enables the formation of dark lines along the outline. The intensity contrast between the interior of the square and the black outline is roughly 15. Actually, the contrast will decrease as the phase jump decreases. Inspired by Reviewer's comments, we have added an additional experiment to demonstrate differentiation on phase image with other phase jumps. For this, we have added a new section in the Supplementary information. (Seen on Pages 14-15 in the Supplementary information)

"Supplementary Note 8. High-order differentiation operation on phase image.

To demonstrate the effectiveness of the high-order differentiation on phase images, we perform the high-order differentiation on phase images with phase jump π, $\frac{\pi}{2}$, and $\frac{\pi}{3}$. The corresponding experimental observations are illustrated in Supplementary Fig. 7 and Fig. 8, from which we can see that edges with small phase jumps can still be revealed after performing the differentiation operation, which is an advantage of differentiation.

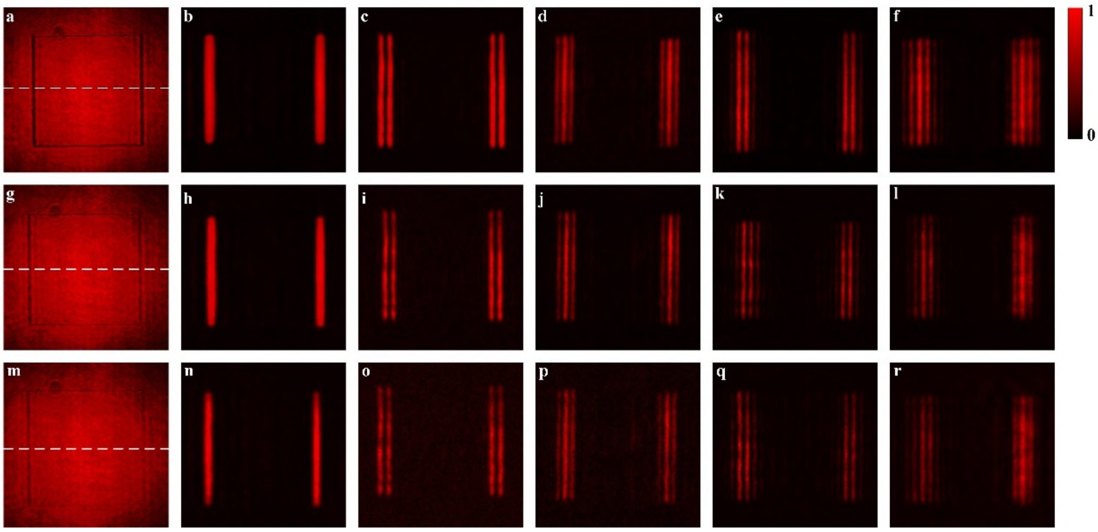

Supplementary Fig. 7. Experimental observations for high-order optical differentiation on phase image with different phase jumps. The first row presents the differentiation on phase square with phase jump π successively from zero-order to fifth-order (from left to right). The second row presents the differentiation on phase square with phase jump $\frac{\pi}{2}$. The third row presents the differentiation on phase square with phase jump $\frac{\pi}{3}$.

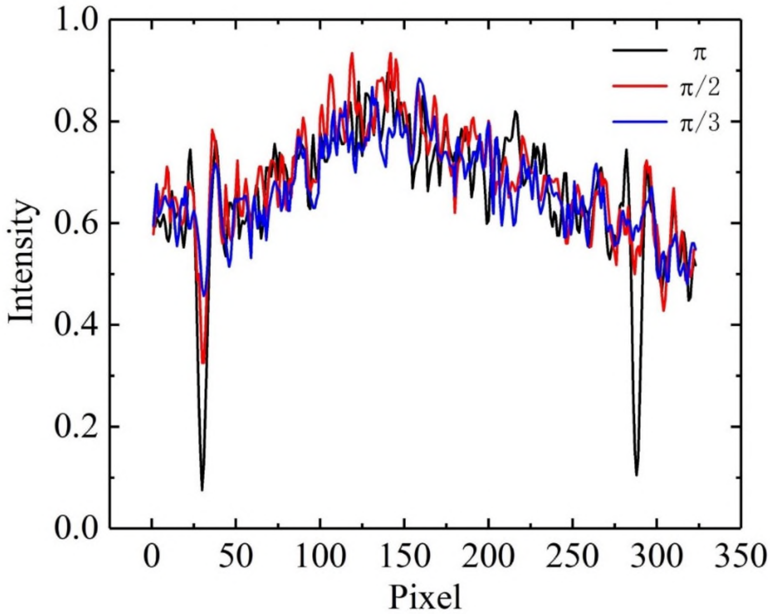

Supplementary Fig. 8. Intensity distributions along white dashed lines in Supplementary Fig. 7. The contrasts, defined by $C = \frac{I_{max}}{I_{min}}$, are calculated as 11.8, 2.9, and 1.9 for the phase jump π, $\frac{\pi}{2}$, and $\frac{\pi}{3}$, respectively.

The corresponding descriptions have also been added to the main text. (Seen on Page 13)

"In our demonstration, the phase jump between the inner and outer of the square is π. Since the phase discontinuity at the edges of a general image can take arbitrary values, in Supplementary Note 8, we perform high-order differentiation on phase images with different phase jumps."

7. What's the new information we learn from the differentiated images vs bright field images in Supplementary Fig. 1? What's the advantage in differentiation?

Response:

Good questions. As shown in Supplementary Fig. 7, in bright field imaging, the edge of the phase jump gradually becomes more blurred as the phase jump decreases. However, after performing the differentiation operation, edges with small phase jumps can still be revealed, which is an advantage of differentiation and can also be seen in Supplementary Fig. 1. As marked by the white circles in Supplementary Fig. 1b and c, some onion cell nuclei, which are blurred and indistinguishable in bright-field imaging, are revealed through the differentiation operation. We have clarified this point in the revised Supplementary information. (Seen on Pages 2-3 in the Supplementary information)

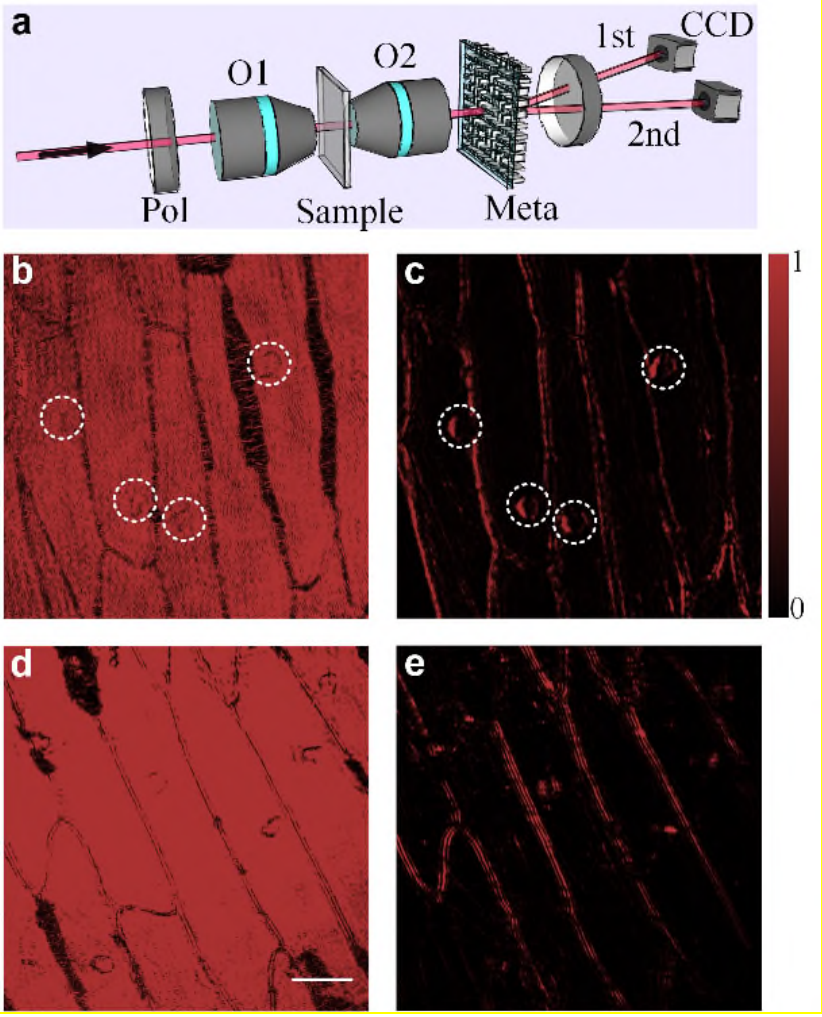

Supplementary Fig. 1. High-order differentiation operations for onion epidermal cells. a illustrates the experimental setup. **b** and **d** the experimental bright filed images of onion epidermal cells. **c** and **e** the corresponding first-order and second-order differentiated images, respectively. The white scale bar represents 100μm. And the magnification of O1 and O2 are 20X and 10X, respectively. White circles are used to mark the onion cell nuclei.

“Compared with the bright-field imaging, after performing the differentiation operation, edges with small phase jumps can still be revealed, which is an advantage of differentiation and can be seen in Supplementary Fig. 1. As marked by the white circles in Supplementary Fig. 1b and c, some onion cell nuclei, which are blurred and indistinguishable in bright-field imaging, are revealed through the differentiation operation."

8. Although the two Gaussian beams are incoherent wrt each other, Eqs. 5 and 6 don't seem to treat them correctly as incoherent beams. It's interesting, then, why the theoretical curves in Fig. 4 agree with the experiment.

Response:

We thank Reviewer for the enlightening comments. Actually, in our demonstration, two independent laser sources are both coherent laser sources. However, since the two lasers are independent, meaning their phases are not synchronized, thereby there is no interference between them. Namely, they are incoherent with respect to each other. In this regard, the signal detected by the power meter can be expressed as,

$$P = P_1 + P_2 \propto \left| exp\left(-\frac{d_1^2}{4\sigma_1^2}\right) H_n\left(-\frac{d_1}{2\sigma_1}\right)\right|^2 + \left| exp\left(-\frac{d_2^2}{4\sigma_2^2}\right) H_n\left(-\frac{d_2}{2\sigma_2}\right)\right|^2, \qquad \text{(R1)}$$

the superscripts 1 and 2 represent the two laser sources, respectively. In our manuscript, one of the lasers, i.e., laser 1, is firstly aligned with the metasurface, which leads to P_1=0. Thus, we obtain the formula (8). ***In this regard, these formulas exactly correspond to our actual experimental situation. This explains why the theoretical curves in Fig. 4 agree with the experiment.*** If two laser sources are coherent with each other, the signal should be expressed as,

$$P = P_1 + P_2 \propto \left| exp\left(-\frac{d_1^2}{4\sigma_1^2}\right) H_n\left(-\frac{d_1}{2\sigma_1}\right) + exp\left(-\frac{d_2^2}{4\sigma_2^2}\right) H_n\left(-\frac{d_2}{2\sigma_2}\right)\right|^2, \qquad \text{(R2)}$$

We have clarified this point in our revision. (Seen on Page 15 in the main text)

"Note that, here, two independent lasers sources are both coherent. However, since the two lasers are independent, meaning their phases are not synchronized, and thus there is no interference between them, namely, they are incoherent with respect to each other."

Inspired by Reviewer 4 and Reviewer 2, we have added a new section in the

Supplementary Information to discuss the situations of incoherent and coherent illumination. (Seen on Pages 9-12 in the Supplementary information)

"Supplementary Note 6. Optical super-resolution with unknown incoherent and coherent illumination.

In the main text, we use two independent laser sources for optical alignment, which are incoherent with respect to each other. Note that the intensity and number of the lasers are known in advance. In some practical applications, the intensity and number of point sources may be unknown, and the light source could be incoherent, such as the incoherent imaging and fluorescence microscopy. To simplify, here, we take the one-dimensional case as an illustrative example. Assume that there are n unknown point sources distributed along the x-axis, and their positions can be expressed as d_i. For each point source, after passing through the metasurface, the resultant incoherent light can be expressed as,

$$E_{i,m} = A_i c_m G(x - d_i) H_m\left(\frac{x-d_i}{\sqrt{2}\sigma}\right), \tag{S1}$$

where $G(x - d_i)$ is the Gaussian function, which is exactly the transfer function of a point source, as indicated in the main text, and A_i is the amplitude of point source *i*, *m* is the order of Hermite polynomial and also corresponds to the order of differentiation, and c_m is the constant coefficient of *m*-order differentiation. Being different from the coherent illumination, in order to acquire the component of fundamental mode with incoherent source, we routinely need to perform ensemble averaging[1], namely,

$$P_{i,m} = \iint \langle E_{i,m}(x_1) G(x_1) E_{i,m}^*(x_2) G(x_2) \rangle \, d_{x_1} d_{x_2}. \tag{S2}$$

According to the property of incoherent, namely,

$$\langle E_{i,m}(x_1) G(x_1) E_{i,m}^*(x_2) G(x_2) \rangle = \left| E_{i,m}(x_1) G(x_1) \right|^2 \times \delta(x_1 - x_2). \tag{S3}$$

In this regard, Eq. (S2) can be expressed as,

$$P_{i,m} = I_i \left| c_m \right|^2 \int \left| G(x - d_i) H_m\left(\frac{x - d_i}{\sqrt{2}\sigma}\right) \right|^2 \left| G(x) \right|^2 dx, \tag{S4}$$

which is exactly similar to the incoherent imaging system in Fourier optics[2]. By leveraging the integral formula,

$$\int_{-\infty}^{\infty} exp[-(x-y)^2]\, H_m(\alpha x) H_n(\alpha x) dx$$

$$= \pi^{\frac{1}{2}} \sum_{k=0}^{min(m,n)} 2^k k! \binom{m}{k}\binom{n}{k} (1-\alpha^2)^{\frac{m+n}{2}-k} H_{m+n-2k}\left[\frac{\alpha y}{(1-\alpha^2)^{\frac{1}{2}}}\right], \qquad \text{(S5)}$$

we conclude that,

$$P_{i,m} \propto I_i \sum_{k=0}^{m} 2^k k! \binom{m}{k}\binom{m}{k} (1-\alpha^2)^{m-k}\, exp\left(-\frac{d_i^2}{2\sigma^2}\right) H_{2m-2k}\left[\frac{-\sqrt{6}d_i}{6\sigma}\right]. \qquad \text{(S6)}$$

Considering all unknown point sources, for *m*-order differentiation, the total signal can be expressed as,

$$P_m = \sum_{i=1}^{n} P_{i,m}. \qquad \text{(S7)}$$

After performing a series of high-order differentiation operations, the positions and intensities of the unknown point sources are embedded in the coefficients of the Hermite polynomials, which subsequently influence the intensity of P_m. It is similar to computational ghost imaging[3], where a series of spot patterns with specific spatial distributions, such as Laguerre-Gaussian modes, Hermite-Gaussian modes, and Hadamard orthogonal matrices, are successively used to illuminate the object. The transmitted or reflected light intensity from the object is then detected by a bucket detector. This intensity corresponds to the coefficients of the corresponding modes, which are subsequently processed to recover the information of the object under test. Accordingly, based on Eq. (6) and Eq. (7), the positions and intensities of the unknown point sources can be estimated. However, it's hard to obtain a clear analytical expression. Some advanced inverse solving algorithms or neural networks can be used to tackle this issue.

If the light source is coherent, namely, these unknown point sources are coherent with each other, such as the coherent imaging, this problem is exactly consistent with the computational ghost imaging or state tomography. Specifically, based on the Eq. (8) in the main text, for each point source and a certain differentiation operation, the signal induced by the proposed super-resolution device can be expressed as,

$$B_{i,m} \propto A_i\, exp(i\varphi_i)\, exp\left(-\frac{d_i^2}{4\sigma^2}\right) H_m\left(-\frac{d_i}{2\sigma}\right), \qquad \text{(S8)}$$

where $A_i\, exp(i\varphi_i)$ represents the complex amplitude of the point source *i*. Considering all unknown point sources, for *m*-order differentiation, the total signal can be expressed as,

$$B_m \propto \sum_{i=1}^{n} B_{i,m}. \tag{S9}$$

If we consider the unknown point sources as a continuously varying image or wavefunction $f(x)$, Eq. (S9) can be expressed as,

$$B_m \propto \int A_i\, exp(i\varphi_i)\, exp\left(-\frac{d_i^2}{4\sigma^2}\right) H_m\left(-\frac{d_i}{2\sigma}\right) d(d_i). \tag{S10}$$

The above overlap integral is exactly consistent with the mode filtering in structured light[4]. If we acquire the value of B_m, the distribution of the unknown point sources can be revealed by,

$$f(x) = \sum_m B_m\, exp\left(-\frac{x^2}{4\sigma^2}\right) H_m\left(-\frac{x}{2\sigma}\right). \tag{S11}$$

Actually, B_m is a complex value. However, in the experiment, the power meter can merely acquire the intensity information, namely, $|B_m|^2$. In order to acquire the phase information of B_m, similar to the polarization state reconstruction and state tomography[5], it is necessary to introduce the superposition detection of different-order differentiations. The above theory of coherent and incoherent illumination could have potential applications in super-resolution imaging, and we leave these possibilities in our future studies."

9. Minor comments: The manuscript has many grammatical errors. Some texts in some figures are not legible.

Response:

We are grateful for Reviewer's careful reading and thorough review. We have consulted a native-speaking colleague to review the manuscript to help address grammatical issues and improve expressions. We have also revised some text in the figures to make them clearer and more readable.

Reviewer 1:

Comment:

I am very satisfied with the efforts the authors made to improve the manuscript.

The significantly revised manuscript can be accepted as is.

Response:

We thank Reviewer for the careful reading and positive recommendations.

Reviewer 2:

<u>Comment:</u>

The authors have responded to all my comments and made revisions accordingly in the manuscript. The paper is in much better shape now. Only one more point for the authors to check:

It is shown by the authors that not only the relative distance between the two lasers ($d=d1-d2$) but also the absolute distances between these lasers and the metasurface ($d1$, $d2$) are important. And it is said that the laser 1 is firstly aligned with the metasurface, namely $d1=0$. I am concerned about the accuracy of this preconditional alignment of laser 1 and the metasurface. Could the author deliberately set $d1 \neq 0$ and be comparable to $d2$ (i.e. $d1 \sim= d2$), and then check whether equation R1 or R2 is still the right formula?

Response:

We appreciate Reviewer for carefully reading our previous response and providing this constructive comment. Since the two lasers are incoherent with each other, the signal detected by the detector is the sum of the light intensities from the two lasers. Namely, the general formula can be expressed as

(R1)

Here, we take the first-order differentiation as an example. Using angular spectrum theory, as indicated by the discrete points in Fig. R1, we numerically simulated the entire optical propagation process (illustrated in Fig. 4a in the main text) and calculated the detected signal. The corresponding prediction from Eq. (R1) is indicated by the red lines. The consistency between them indicates that Eq. (R1) holds true for $d_1 \neq 0$. We sincerely appreciate the reviewer's concern regarding **the accuracy of the preconditional alignment of laser 1 and the metasurface**. From Fig. R1, we can see that, d_1 can be determined by the intensity of the background signal, which is the intensity detected by the detector when $d_2=0$. This can also be seen as a special case of optical super-resolution with unknown illumination in Supplementary Note 6.

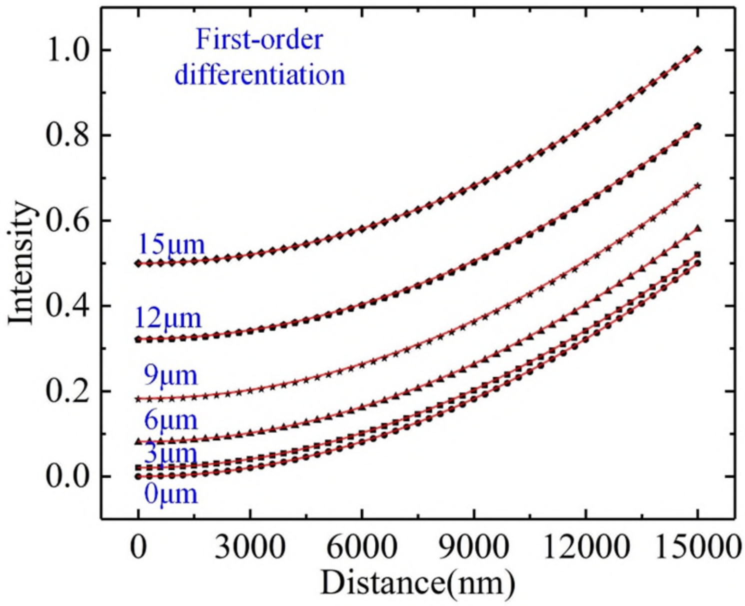

Fig. R1. Numerical simulation of Eq. (R1) with $d_1 \neq 0$. The beam waist is set as 70μm. The value of d_1 is set from 0 to 15μm, with a step size of 3μm. The x-axis is the distance of laser 2 from the center of the metasurface, i.e., d_2.

Inspired by Reviewer's comments, we have added some remarks in our revision (seen on page 18 in the main text)

"In theory, our method can be extended to determine the absolute distance of laser 1 and laser 2 from the metasurface, namely, optical super-resolution with unknown illuminations, as discussed in Supplementary Note 6."

By addressing the Reviewer's concerns, we indeed feel that our manuscript has been much improved and can effectively avoid confusion. We sincerely wish Reviewer could consider the manuscript for publication in Nature Communications.

Reviewer 3:

Comment:

I co-reviewed this manuscript with one of the reviewers who provided the listed reports. This is part of the Nature Communications initiative to facilitate training in peer review and to provide appropriate recognition for Early Career Researchers who co-review manuscripts.

Response:

We thank Reviewer for the co-review.

Reviewer 4:

Comment:

I have reviewed the revised manuscript and don't have additional comments.

Response:

We thank Reviewer for the careful reading and positive recommendations.

Reviewer 2:

Comment:

The authors have addressed the comments raised.

Response:

Thank you very much again for taking the time to review our manuscript and for the insightful suggestions you provided for our article.

Reviewer 3:

<u>Comment:</u>

I co-reviewed this manuscript with one of the reviewers who provided the listed reports. This is part of the Nature Communications initiative to facilitate training in peer review and to provide appropriate recognition for Early Career Researchers who co-review manuscripts.

Response:

We thank Reviewer for the co-review.